ACS Partner Journal
PRECISION CHEMISTRY
pubs.acs.org/PrecisionChem

Review

Recent Progress in Electrocatalytic Conversion of Lignin: From Monomers, Dimers, to Raw Lignin

Xiang Liu, Ye Wang, and Haohong Duan*

Cite This: *Precis. Chem.* 2024, 2, 428−446

Read Online

ACCESS | Metrics & More | Article Recommendations

ABSTRACT: Lignin, as the second largest renewable biomass resource in nature, has increasingly received significant interest for its potential to be transformed into valuable chemicals, potentially contributing to carbon neutrality. Among different approaches, renewable electricity-driven biomass conversion holds great promise to substitute a petroleum resource-driven one, owing to its characteristics of environmental friendliness, high energy efficiency, and tunable reactivity. The challenges lie on the polymeric structure and complex functional groups in lignin, requiring the development of efficient electrocatalysts for lignin valorization with enhanced activity and selectivity toward targeted chemicals. In this Review, we focus on the advancement of electrocatalytic valorization of lignin, from monomers, to dimers and to raw lignin, toward various value-added chemicals, with emphasis on catalyst design, reaction innovation, and mechanistic study. The general strategies for catalyst design are also summarized, offering insights into enhancing the activity and selectivity. Finally, challenges and perspectives for the electrocatalytic conversion of lignin are proposed.

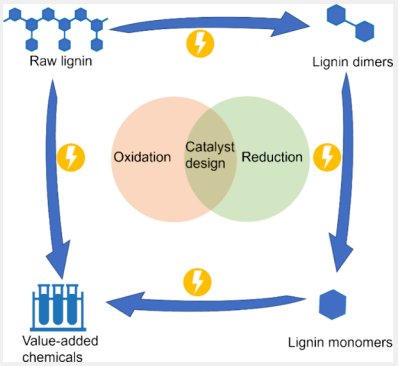

KEYWORDS: *Lignin, Electrocatalytic oxidation, Electrocatalytic reduction, Electrocatalyst design, Selectivity regulation*

1. INTRODUCTION

The depletion of fossil fuels with the rapid development of modern society has led to a more serious environmental crisis, calling for increasing demand for clean and green energy. Therefore, it is crucial to develop technologies for the production of chemicals from renewable resources, in which biomass represents an important alternative.[1] As the second largest biomass resource after cellulose in nature, lignin serves as a crucial structural component in plant cells. Lignin is often produced as industrial byproducts in the paper industry (50 million per year), waste crops, and biofuel refineries industry (75 million per year) with huge yields, the efficient utilization of which will contribute to achievement of carbon neutral goals (Figure 1a).[2,3] It is predominantly employed as a stabilizer, emulsifier, and binder in the industrial sector by directly utilizing modified macromolecules due to its good dispersion, adhesion, and surface activity.[4]

Parallel with these conventional applications, increasing attention lies in catalytically converting lignin to valuable chemicals, taking advantage of the unique structure of lignin (Figure 1b). The polymeric structure of lignin consists of three types of phenolic derivatives as monomers, including *p*-coumaryl alcohol, coniferyl alcohol, and sinapyl alcohol, which are phenylpropanoid units and can be degraded to phenol, guaiacol, and syringol, respectively. These monomers are connected by various ether and carbon−carbon linkages,[2,5] in which ether linkages such as β-O-4 bonds, α-O-4 bonds, and 4-O-5 bonds account for more than 70% of the connection modes, and nonpolar and stable carbon−carbon bonds such as β-5 bonds, $\beta-\beta$ bonds, and 5−5 bonds occupy the remainng 30%. Due to its abundant carbon source and unique structure, lignin represents a potential alternative to fossil resources to produce valuable chemicals.[6,7] However, the recalcitrant polymeric structure and complex functional groups remain as challenges for achieving selective conversion of lignin. Thermocatalysis facilitates the deoxygenation of lignin monomers and even raw lignin to yield arenes, but this process often necessitates relatively high reaction temperatures (>200 °C) and high hydrogen pressures (0.7−5 MPa).[8−10] Photocatalysis has emerged as a sustainable method for cleavage of various bonds in lignin dimers,[11−14] but still suffers from low activity. Enzymatic catalysis offers environmentally friendly processes and high product selectivity, but is restricted by the high operation costs and susceptibility to inactivation of enzyme catalysts.[15,16] Compared with thermo-, photo-, and enzymatic-catalysis, electrocatalysis stands out due to the environmental friendliness by utilizing renewable electricity. The mild

Received: March 26, 2024
Revised: May 26, 2024
Accepted: May 27, 2024
Published: June 6, 2024

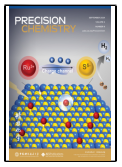

https://doi.org/10.1021/prechem.4c00024
Precis. Chem. 2024, 2, 428−446

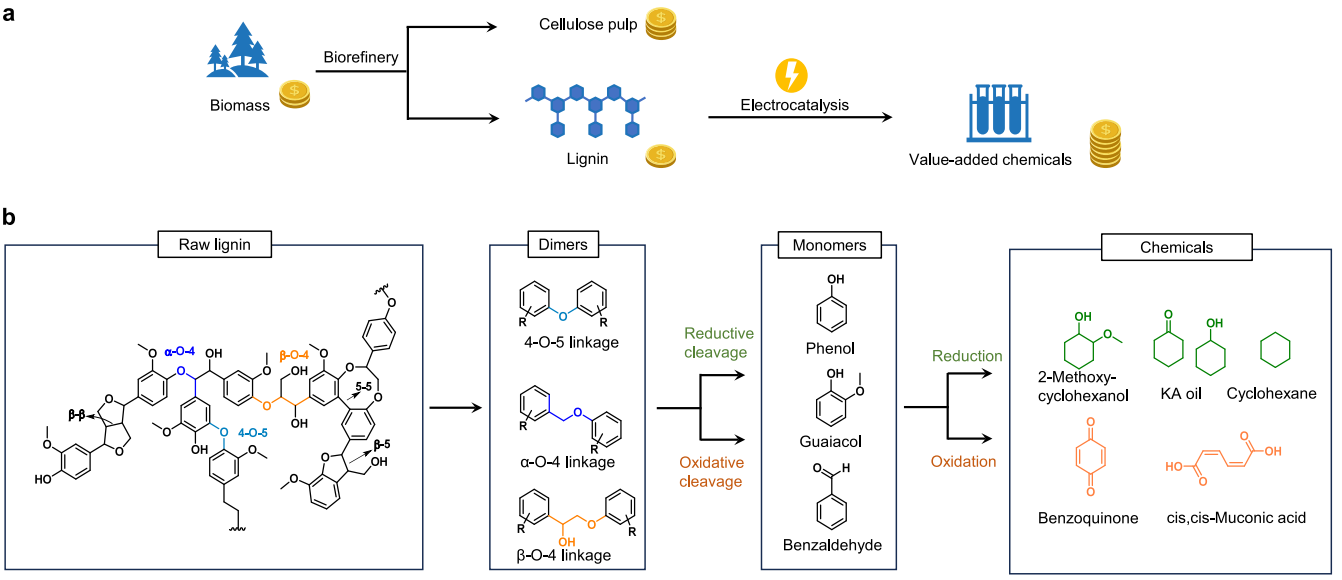

Figure 1. (a) Scheme of lignin production and the electrocatalytic refinery. (b) Schematic pathway of lignin to chemical products by electrocatalysis.

operating conditions and efficient energy conversion render it an appealing option for chemical production. In addition, the electrocatalytic devices exhibit simplicity and high modularity, thereby reducing the construction and maintenance costs of the reaction system.

Last, electrocatalysis demonstrates significant tunability in terms of activity and selectivity by varying applied potentials, electrolytes, and catalysts. Particularly, a range of strategies have been developed, including potential adjustment, electrolyte composition optimization, and catalyst design, toward achieving efficient production of target compounds. Therefore, it is promising to explore the value-added conversion of lignin via electrocatalysis.

The development of electrocatalytic strategy for organic compounds conversion is rapid, especially the upgrading biomass-derived polyols and furans.[17−23] In contrast, research progress in the electrocatalytic upgrading of lignin is relatively sluggish due to the polymeric structure and complex functional groups. Specifically, owing to its high molecular weight and presence of hydrophobic groups, lignin and many of its derived compounds exhibit limited solubility in aqueous solution and steric hindrance, showing weak interaction with an electrode, which results in a reduced reactivity and side reaction such as water splitting in an aqueous medium; furthermore, the intricate functional groups and structural units deliver diverse array of products from degradation of lignin, thereby posing challenges for selectivity control and associated downstream products separation and purification processes. As a result, studies on the electrocatalytic conversion of lignin typically commence with lignin monomers and dimers. Although several reviews have summarized the advancements in the electrocatalytic reduction of lignin monomers and dimers, as well as the oxidation of lignin dimers through hydrogen atom transfer (HAT) mediators, insufficient notice has been given to the progress in electrocatalytic oxidation strategy, the conversion of raw lignin, and the design of electrocatalysts.[24−26] Moreover, exciting achievements regarding catalyst design for electrocatalytic lignin conversion have been witnessed in recent years, which is probably benefited from the progress in catalyst synthesis method, characterization and mechanism understanding in a more precise fashion.[27−32] Hence, it is imperative to undertake a review on advanced catalyst design for electrocatalytic conversion of lignin.

In this Review, we provide a comprehensive summary of electrocatalytic conversion of lignin from simple monomer to dimer and then to complex raw lignin (Figure 1b), including both reduction and oxidation strategies and covering recent significant advancements in catalyst design. We first present the electrocatalytic conversion of lignin monomers, primarily phenol and guaiacol, including electrocatalytic hydrogenation (ECH), hydrodeoxygenation, and oxidation. Moreover, we introduce the electrocatalytic selective cleavage of lignin dimers, by either reductive or oxidative strategies. Then, we shift our focus to the electrocatalytic degradation of raw lignin. Considering the importance of electrocatalysts in facilitating the above conversion reactions, we then delve into electrocatalyst design strategies. Finally, we propose future prospects for electrocatalytic lignin valorization.

2. LIGNIN MONOMERS: SELECTIVE CONVERSION

2.1. Hydrogenation

Electrochemical hydrogenation (ECH) has aroused wide interest in the reduction of organic compounds that hydrogenate organic compounds via a HAT process using adsorbed hydrogen atoms (H_{ads}) or a direct proton-coupled electron transfer (PCET) process. Specifically, the HAT mechanism involves the following steps: (1) Volmer step, which is a proton-coupled electron transfer (PCET) process at the active sites over the metal electrodes, by which H_{ads} is generated; (2) adsorption of organic compounds onto the metal sites on the electrode; (3) hydrogenation of the organic compounds by H_{ads}; and (4) desorption of the hydrogenated organic compounds. The PCET mechanism involves the following steps: (1) Adsorption of organic compounds onto the metal sites on the electrode; (2) direct hydrogenation via a PCET process; (3) desorption of the hydrogenated organic compounds. Notably, the hydrogen evolution reaction (HER) is the main competitive reaction with the ECH of organic compounds, which mostly takes place through a Volmer−Heyrovsky or Volmer−Tafel mechanism as follows: (1) Volmer step, which is the same as the first step in the ECH process; (2) Heyrovsky step, which is also a PCET process

https://doi.org/10.1021/prechem.4c00024
Precis. Chem. 2024, 2, 428−446

or Tafel step which is a recombination process of H_{ads} and H_{ads} without the involvement of electron transfer.[33]

2.1.1. Phenol. Due to the complexity of the lignin structure, model compounds are always adopted in fundamental research. Phenol serves as a suitable model monomer for investigating the electrocatalytic valorization of lignin. The ideal hydrogenated products of phenol are cyclohexanone and cyclohexanol (that is overall called KA oil), which can be employed as important organic solvents and chemical upstream raw materials for the production of adipic acid and cyclohexanone oxime with wide applications in nylon and plastic industries (Scheme 1).[34]

Scheme 1. Value-Added Products for Hydrogenation of Lignin Monomers

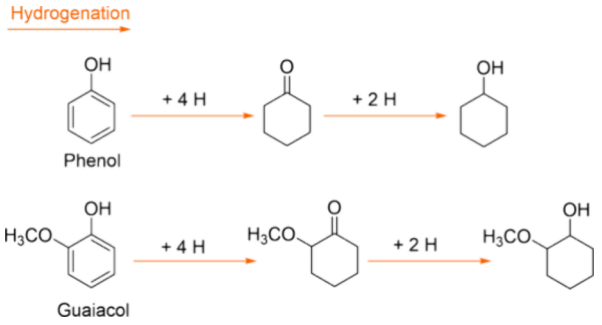

Previous studies have demonstrated that noble-metal electrocatalysts, such as platinum (Pt), palladium (Pd), ruthenium (Ru), and rhodium (Rh), exhibit exceptional HER activity and can be also employed for the ECH process of phenol.[35−37] The production of cyclohexanone, the semihydrogenation product of phenol, was more pronounced when the conversion of phenol was relatively low. However, noble-metal catalysts with single component exhibited certain limitations, including low current density (<10 mA cm^{-2}) and low cyclohexanone selectivity. Mechanism studies indicated that the phenol ECH process followed a Langmuir−Hinshelwood mechanism.[38] The rate-determining step (RDS) was the thermochemistry reaction between adsorbed phenol and H_{ads}, evidenced by the zero-order relationship between the phenol concentration and reaction rate at different currents. The coverages of phenol and H_{ads} on the electrode surface were a significant factor affecting the faradaic efficiency (FE) of ECH. Under a more negative potential, the Volmer step on the catalyst surface was intensified, leading to an augmentation in H_{ads} coverage, which in turn amplified HER and thus diminished the FE of ECH process products, that is, cyclohexanone and cyclohexanol. The increase in temperature could accelerate the reaction rate of RDS and consequently enhance FE to a certain extent; however, the magnitude of this improvement remained limited.

Recently, Han and co-workers conducted a comprehensive study of a series of alloy catalysts supported on nitrogen-doped hierarchically porous carbon (NHPC) for ECH of phenol (Figure 2a).[31] Among the different alloy catalysts, Pt-based catalysts exhibited superior phenol ECH performance and tunable product selectivity. Moreover, a nickel-modified Pt catalyst (NiPt/NHPC) showed high selectivity of cyclohexanone (over 99%) in a 0.5 mol L^{-1} H_2SO_4 solution at room temperature, with the highest production rate of 115.1 mol h^{-1} mol^{-1}; while a RuPt/NHPC catalyst exhibited over 99% selectivity of cyclohexanol, with the highest production rate reaching 213.5 mol h^{-1} mol^{-1}. Density functional theory (DFT) calculations indicated that the excellent selectivity of NiPt/NHPC in catalyzing ECH of phenol to cyclohexanone could be ascribed to its regulated absorption capability for cyclohexanone (Figure 2b). The weaker the adsorption of cyclohexanone, the more favorable the desorption process, thereby effectively suppressing the successive hydrogenation of cyclohexanone to cyclohexanol. Additionally, a notable aspect of this study lies in the simultaneous conversion of phenol at both the cathode and anode, leading to the formation of cyclohexanone and benzoquinone, respectively (Figure 2a). The anode part in this study will be discussed in the latter section of phenol oxidation.

The product selectivity control by electrocatalyst in ECH of phenol was also demonstrated by Zhang and co-workers, who used non-noble Ni nanoparticles (NPs) supported by a molybdenum dioxide (MoO_2) catalyst for effective ECH of phenol.[27] Ni, the active site, was integrated with defective MoO_2 with strong electronic interaction (Figure 2c). The obtained Ni-MoO_2 heterogeneous exhibited enhanced adsorption capability for phenol, which was responsible for the superior ECH FE (~53%) at high conversion (>90%) (Figure 2d, left bottom). As an electron acceptor, MoO_2 exhibited a high density of oxygen vacancies (O_v) on $Ni_{10}@MoO_{2-x}/C$ with a low Ni loading, thereby significantly enhancing the adsorption capacity for cyclohexanone and leading to a high yield of 95% for cyclohexanol (Figure 2d, left). While increasing the Ni content to form $Ni_{20}@MoO_{2-x}/C$ diminished the density of O_v sites, resulting in a high yield of 86% for cyclohexanone (Figure 2d, right).

Furthermore, the catalyst suspension consisting of multiple components can cooperatively improve the catalytic performance. Deng et al. achieved both high FE and high conversion of phenol ECH catalyzed by suspended noble metal catalysts and silicotungstic acid (SiW_{12}).[39] SiW_{12}, a polyoxometalate (POM), serves as a charge storage and hydrogen transfer catalyst, facilitating electron transfer from the cathode to the surface of the catalyst particles (Figure 2e). The suspension system significantly enhanced the diffusion and collision of reactant molecules with the catalyst surface. The phenol conversion exceeded 99% with a selectivity toward cyclohexanol of 90% over suspended Pt/C, while maintaining a cathode current density of 100 mA cm^{-2} and achieving a high FE of 98%. When suspended Pd/C was used as the catalyst, cyclohexanone could be generated with a high selectivity of 95% and a FE of 93% under the same conditions.

In addition to catalyst design, the optimization of electrochemical reactors plays a crucial role in enhancing the product selectivity and current density. Gyenge and co-workers designed a stirred slurry electrochemical reactor (SSER) with the aim of achieving optimal dispersion of the electrocatalyst and enhancing mass transfer between lignin monomers and catalyst particles.[40,41] Figure 2f indicates that the supported catalyst powder was introduced into the solution to create a slurry in this system. The reaction could be conducted at high current densities (>100 mA cm^{-2}), simultaneously effectively suppressing HER. The FE and selectivity in phenol ECH were significantly influenced by varying noble catalysts and the pH of the solutions. The utilization of Pt and Ru catalysts under neutral conditions resulted in a remarkable enhancement in the total FE (>90%) and cyclohexanol selectivity (>90%) during phenol ECH.

2.1.2. Guaiacol. In addition to phenol, various phenol derivatives with alkyl or alkoxy substituents were also extensively

https://doi.org/10.1021/prechem.4c00024
Precis. Chem. 2024, 2, 428−446

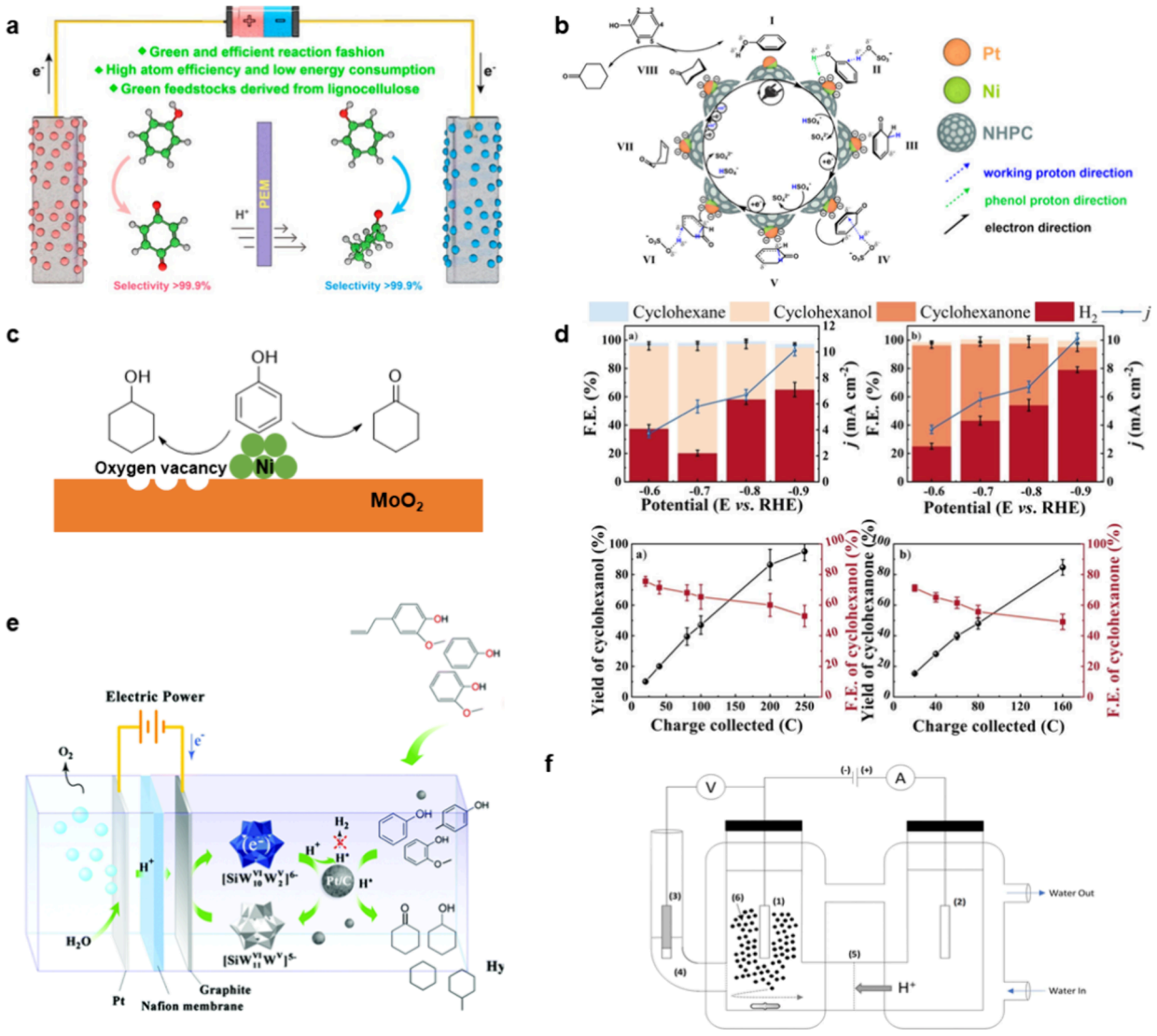

Figure 2. (a) Strategies employed for the electrocatalytic integration of phenol reduction and oxidation. (b) Proposed mechanism of ECH of phenol over the NiPt/NHPC catalyst. Reproduced from ref 31. Copyright 2022 American Chemical Society. (c) Schematic diagram of selective hydrogenation of phenol. (d) Summary of bulk electrolysis results long-term electrolysis results with $Ni_{10}@MoO_{2-x}/C$(left) and $Ni_{20}@MoO_{2-x}/C$ (right). Conditions: 0.1 M H_2SO_4 with 20 mM phenol at 60 °C. Reproduced from ref 27. Copyright 2023 John Wiley and Sons. (e) Schematic illustration of suspended-catalyst electrolysis with SiW_{12}. Reproduced from ref 39. Copyright 2020 Royal Society of Chemistry. (f) Schematic illustration of SSER reactor. Reproduced from ref 41. Copyright 2021 Springer Nature.

investigated as the lignin monomers; one of the representatives is 2-methoxyphenol (that is, guaiacol). Guaiacol usually undergoes concurrent hydrogenation and hydro-deoxygenation reactions under ECH conditions. Therefore, the conversion of guaiacol can yield a range of products, including 2-methoxycyclohexanol, 2-methoxycyclohexanone, phenol, cyclohexanol, and cyclohexanone (Scheme 1, bottom).[40] Among them, methoxylated cyclohexane derivatives with methoxy groups ($-OCH_3$), exhibit notable antimicrobial and anticancer properties. Additionally, these compounds are promising precursors for pharmaceutical applications.[42] In contrast to phenol, the relationship between the concentration of guaiacol and the reaction rate follows a first- or second-order kinetics, suggesting that the RDS is governed by the adsorption of guaiacol on the metal surface due to steric hindrance from substituents, rather than the reaction between adsorbed species.[40] Moreover, the thermodynamic preference for demethoxylation under ECH conditions results in a diminished selectivity toward cyclohexane derivatives.

In a recent work, Sargent, Zhao, and co-workers incorporated gold (Au) into PtRh catalyst to form a ternary PtRhAu electrocatalysts which could selectively hydrogenate lignin monomers to methoxylated cyclohexane derivatives (Figure 3a).[43] The FE of 2-methoxycyclohexanol reached 58% with the partial current density of 116 mA cm^{-2}, which exhibited a significant enhancement in comparison to that over Pt and PtRh. (Figure 3b). Moreover, the PtRhAu catalyst exhibited exceptional stability, with negligible potential decay and minimal decrease in FE over 60 h. The electron structure of Pt was modulated by incorporating Rh and Au with changes in local coordination. The free energy of intermediates on PtRhAu catalyst was effectively manipulated to enhance guaiacol coverage, promote hydrogenation, and inhibit demethoxylation. The optimization of the reactor also exerts a positive effect on the substrate expansion. The above SSER system was applicable

https://doi.org/10.1021/prechem.4c00024
Precis. Chem. 2024, 2, 428−446

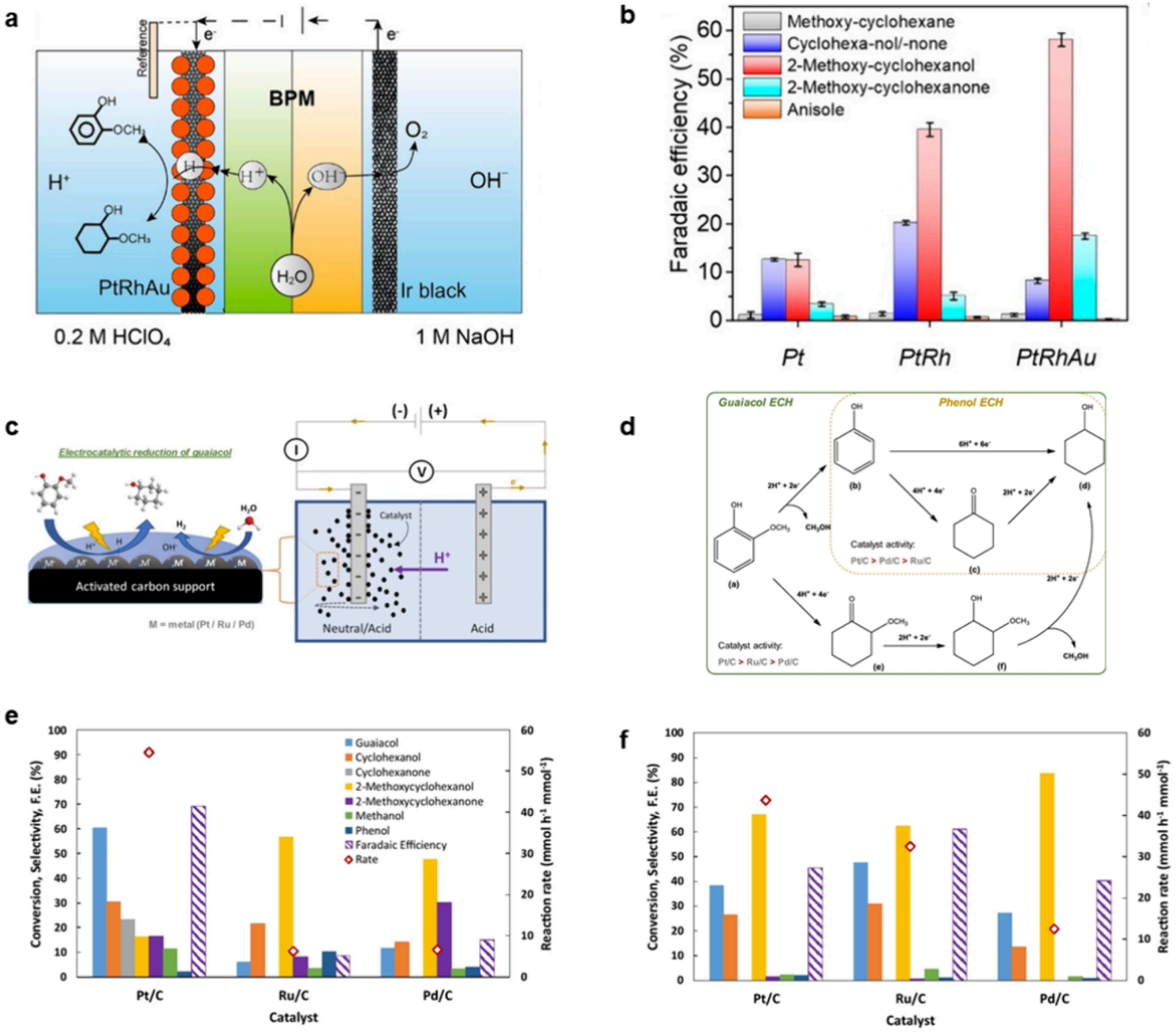

Figure 3. (a) Schematic illustration of a flow-cell system. (b) FE toward various products on Pt, PtRh, and PtRhAu catalysts at 200 mA cm^{-2} for 1 h reaction. Reproduced from ref 43. Copyright 2021 American Chemical Society. (c) Schematic illustration of guaiacol reduction by the SSER reactor. (d) Schematic of the reaction pathways for the guaiacol and phenol ECH and the activity order of the carbon-supported metal catalysts. Compounds: **a** guaiacol, **b** phenol, **c** cyclohexanone, **d** cyclohexanol, **e** 2-methoxycyclohexanone, **f** 2-methoxycyclohexanol, and methanol as the byproduct. Catalytic performance of carbon-supported metals in ECH of guaiacol in (e) acid (0.2 mol L^{-1} H_2SO_4) and (f) neutral (0.2 mol L^{-1} NaCl) at current density of 109 mA cm^{-2}. Reproduced from ref 41. Copyright 2021 Springer Nature.

for ECH of guaiacol (Figure 3c).[41] The complete integration of catalyst slurry and guaiacol significantly enhanced the overall FE. By investigating the product distribution yielded by various catalysts and evaluating the FE of ECH, the ECH pathway of guaiacol was illustrated in Figure 3d. If the initial step of guaiacol reduction involved the demethoxy reaction, phenol was obtained as the intermediate product, which could be selectively hydrogenated to either cyclohexanone or cyclohexanol through the ECH process. Alternatively, if the benzene group was first hydrogenated, 2-methoxycyclohexanone and 2-methoxycyclohexanol would be produced as the intermediates, while further demethoxy reaction led to the production of cyclohexanol. The FE and reaction rate of guaiacol ECH were found to be the highest when utilizing Pt/C catalysts (Figure 3e). Through evaluating pH of the electrolyte, it was demonstrated that the initial hydrogenation of phenyl in guaiacol was favorable under nonacidic conditions, as evidenced by the 2-methoxycyclohexanol reaching the highest selectivity (65%) among the products (Figure 3f).

The integration of catalyst design and reactor optimization can enhance the practical applicability of guaiacol ECH. Zhao and co-workers synthesized carbon felt-supported RhPtRu catalysts which achieved FE of 63% and high selectivity of 91.2% toward methoxy-cyclohexane at current density of 50 mA cm^{-2}.[44] The cleavage of -OCH_3 was also greatly inhibited. Based on this premise, they successfully designed a flow-cell system to achieve an industrial current density exceeding 400 mA cm^{-2} using Rh-covered PTFE electrodes, while also obtaining a significant 57.8% FE to methoxylated cyclohexane derivatives.[30] The high permeability of Rh diffusion electrodes to electrolytes

https://doi.org/10.1021/prechem.4c00024
Precis. Chem. 2024, 2, 428−446

was crucial for enhancing the FE and decreasing the flow-cell voltage.

2.2. Hydrodeoxygenation

2.2.1. Phenol. In addition to hydrogenation, lignin monomers can undergo the hydro-deoxygenation process under ECH conditions (Scheme 2). However, the higher activation energy of hydrodeoxygenation than HER makes the electrocatalytic deoxidation under mild conditions difficult. Deng and co-workers achieved the conversion of phenol to cyclohexane in the suspended Pt/C and SiW_{12} system.[39] The DFT calculation results revealed the reaction mechanism from phenol to cyclohexane (Figure 4a). Initially, hydrogenation of phenol occurred on the surface of a Pt catalyst, resulting in the generation of cyclohexanol. Subsequently, the superacidic property of SiW_{12} facilitated the protonation and dehydration of cyclohexanol, ultimately resulting in its conversion into cyclohexane via reduction utilizing POM-H (Figure 4b). The increase in temperature and current densities promoted the formation of the deoxidation product, cyclohexane; however, the overall selectivity of cyclohexane was relatively low (18.6% at 800 mA cm^{-2} and 55 °C), which requires further improvement (Figure 4c).

Scheme 2. Value-added products for hydrodeoxygenation of lignin monomers

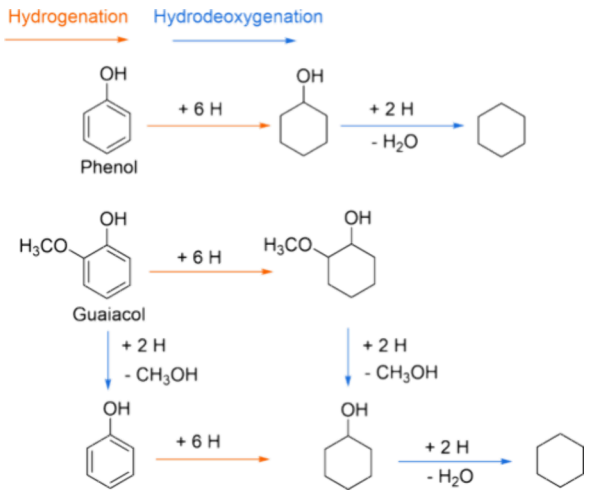

2.2.2. Guaiacol. The enhancement of selectivity toward one certain product in the guaiacol electroreduction is crucial for its practical application. One possible route for the demethoxylation of guaiacol is the formation of cyclohexanol or cyclohexanone. SSER system could achieve the selective conversion of guaiacol to cyclohexanol under optimized conditions.[40] Product distribution over Pt/C was influenced by synergistic interaction effects among the major experimental conditions, including proton concentrations, temperatures, and cathodic current densities, which, in turn, affected the surface coverage of H_{ads}. The FE of phenol electroreduction and the selectivity of cyclohexanol can be enhanced through a pH reduction in the electrolyte (Figure 4d). Although increasing the current density can enhance the selectivity of hydrodeoxygenation, it will concurrently diminish the FE (Figure 4e). Elevating temperatures could promote the demethoxylation of guaiacol, thus impeding the phenyl hydrogenation process and diminish-

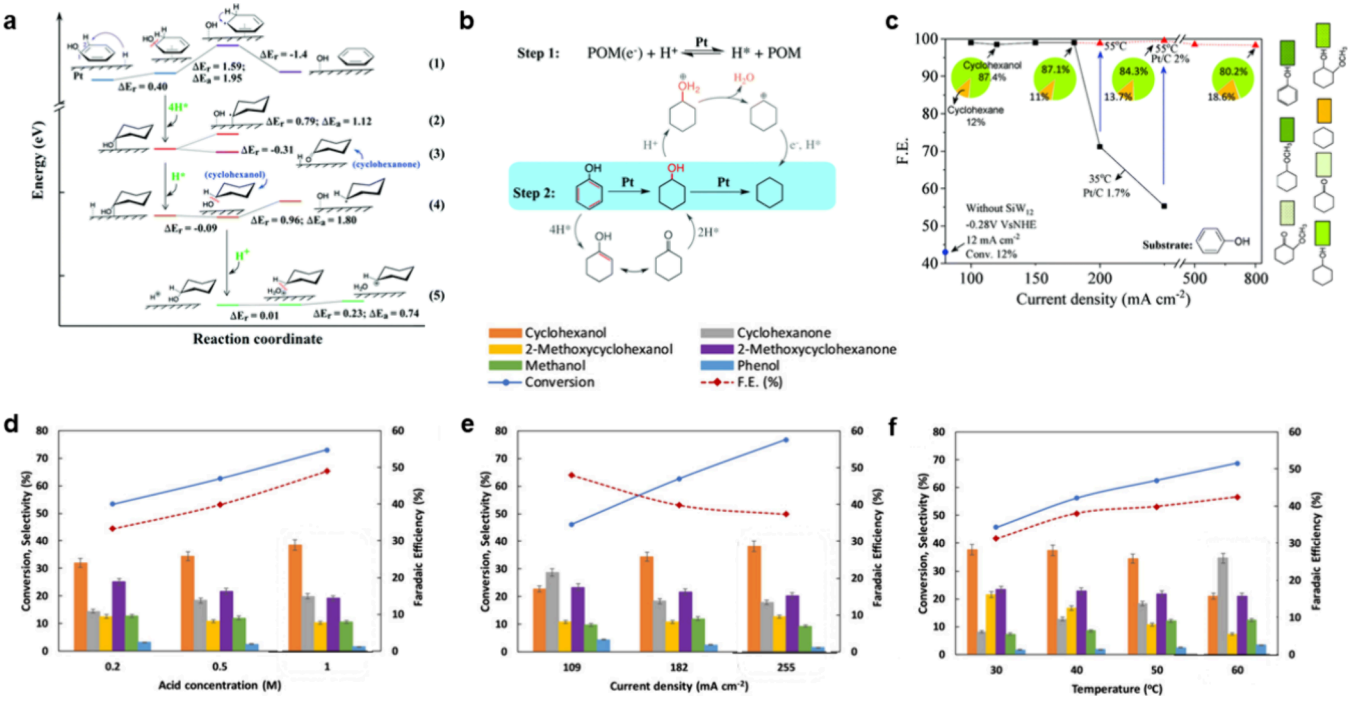

Figure 4. (a) Energy diagram of phenol hydrogenation and deoxygenation over Pt(111) with solvation model computation. (b) Schematic representation of the possible reaction pathways of phenol in the electrolytic hydro-deoxygenation. (c) FE changes and product distributions in the phenol electrolysis under different current densities at the suspended Pt/C and SiW_{12} system. Reproduced from ref 39. Copyright 2020 Royal Society of Chemistry. Effect of (d) acid concentrations at 50 °C and 109 mA cm^{-2}, (e) superficial cathodic current density in 0.5 mol L^{-1} H_2SO_4 at 50 °C, and (f) temperatures in 0.5 mol L^{-1} H_2SO_4 at 109 mA cm^{-2} over Pt/C on the ECH of guaiacol after 5 h of electrolysis. Reproduced from ref 40. Copyright 2020 John Wiley and Sons.

https://doi.org/10.1021/prechem.4c00024
Precis. Chem. 2024, 2, 428−446

ing the formation of the 2-methoxycyclohexanone intermediate (Figure 4f).

As previously mentioned, the dual-catalyst suspension system developed by Deng et al. exhibited a robust reduction capability, with the detection of cyclohexane in the process of phenol ECH. For ECH of guaiacol, the suspended Pt/C and SiW_{12} system reached a 56% selectivity of cyclohexanol at 150 mA cm^{-2}, while exhibiting minimal hydrogen production.[39] Moreover, the reduction product distributions of guaiacol in this system exhibited negligible variation with respect to changes in the current density. The increase in reaction temperature from 35 to 55 °C was demonstrated to enhance the overall FE from 65% to 98% at high current densities of 250 mA cm^{-2} (Figure 4c). This suspended system exhibited universally satisfactory electroreduction properties of lignin monomer derivatives.[45]

2.3. Oxidation

2.3.1. Phenol. Although there has been extensive research and advancement in the electrochemical hydrogenation of lignin monomers, studies on the electrooxidative valorization of these monomers remain limited (Scheme 3). The electrocatalytic

Scheme 3. Value-Added Products for Oxidation of Lignin Monomers

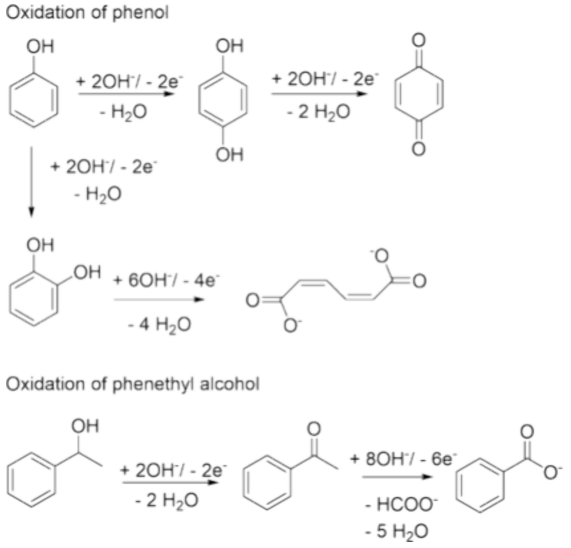

oxidation of phenol can yield hydroquinone (HQ), catechol, and *p*-benzoquinone (BQ); however, the selectivity control over these products remains a challenge due to the possibility of overoxidation, inevitably resulting in the generation of various byproducts including maleic acid, oxalic acid, formic acid, and carbon dioxide.[46,47]

The oxidation of phenol to BQ on the Pt electrode at optimized potentials was reported, affording a yield of approximately 43% for BQ.[46] Waldvogel et al. employed a Ruiridic oxide (IrO_2) electrode in a methyl cyanide-methanol-H_2O solution, facilitating the selective conversion of phenols into BQ with high yields up to 99%, albeit at a significantly low current density of 2 mA cm^{-2}.[48] Through extensive screening of alloy catalysts, Han et al. discovered that NHPC-supported FeRu catalyst exhibited a phenol conversion of 43% and selectivity greater than 99.9% in the oxidation of phenol to BQ.[31] The outstanding electrocatalytic performance of the catalysts could be attributed to the limited adsorption capacity of NiPt alloy NPs toward cyclohexanone and single-atom Fe decorated Ru NPs toward BQ, thereby preventing overoxidation of the desired products.

In addition to heterogeneous catalysis, Zhang et al. presented a homogeneous electrochemical strategy for the selective conversion of phenol into BQ using a cocatalytic redox partner comprised of simple transition-metal ions of cobalt(III) ions (Co^{3+}) and cupric ion (Cu^{2+}).[49] The selectivity of BQ, however, remained below 70%, which could be further improved.

2.3.2. Catechol. Presenting a novel perspective on the oxidative valorization of lignin monomers, Gong and co-workers developed electrooxidation of 2-hydroxyphenol (catechol) to *cis,cis*-MA over a facilely prepared cupric oxide (CuO) foam anode with a hydrogen-evolving cathode in an alkaline aqueous solution (Figure 5a).[28] The addition of zinc ion (Zn^{2+}) greatly enhanced the formation of *cis, cis*-products and inhibited monomers repolymerization due to the coordination between Zn^{2+} and two catechol molecules (Figure 5b), thus reaching high yield (90%) and selectivity (87%) of *cis,cis*-muconate reached under ambient conditions (Figure 5c). The applicability of the Zn^{2+} strategy can be extended to other typical electrodes (such as carbon paper and Cu foam). In addition to Zn^{2+}, the introduction of other cations also leads to an increase in the FE; however, it is accompanied by a reduction in the yield. This could be attributed to the strong tendency of forming stable hydroxide solids or hydroxide complexes in alkaline environments.

2.3.3. Other Lignin Monomers. In addition to the aforementioned lignin monomers, there are also monomers that retain linkage structures. Phenethyl alcohol (**1**) and its derivatives are lignin monomers containing β-O-4 linkages, wherein the C(OH)-C bond possesses the potential to undergo cleavage, leading to the formation of carboxylic acid derivatives. Our group reported an efficient strategy for the selective upgrading of derivatives of **1** by a manganese-doped cobalt oxyhydroxide electrocatalyst supported on nickel foam (MnCoOOH/NF).[32] The strategy not only enabled the generation of carboxylate at the anode but also concurrently mitigated the overpotential of water splitting, leading to a great enhancement in hydrogen production rate at the cathode (Figure 5d, e). The pathway of **1** involved the oxidation of the hydroxyl group on C_α first and the cleavage of the C_α-C_β bond subsequently. Compared with other catalysts, MnCoOOH exhibited enhanced capability in cleaving the C_α-C_β bond and great versatility to different substrates, leading to an "electrochemical funnel" for benzoate production (Figure 5f, g). The detailed mechanism of Mn-doping will be discussed later in "5.2. Heteroatom doping strategy".

3. LIGNIN DIMERS: SELECTIVE CLEAVAGE

Based on the linkages between lignin monomers, there are several typical dimers in lignin: the phenyl benzyl ether represents a fundamental structural unit of the β-O-4 linkage, with diphenyl ether standing for the simplest structure for the α-O-4 linkage. The hydrogen on the phenyl group can be substituted by hydroxyl and carbonyl groups to achieve a closer resemblance to the authentic structure of lignin. Nonpolar carbon−carbon bonds such as β-1, β-5, and β−β linkages are extremely stable, so the dimers have poor cleavage reactivity. Previous studies focused on developing efficient catalysts or reaction systems in cleaving these linkages in dimers, which is a pivotal step for further study about the depolymerization of lignin. From the perspective of reaction types, the reaction mechanisms of the electrocatalytic cleavage of lignin dimers can

https://doi.org/10.1021/prechem.4c00024
Precis. Chem. 2024, 2, 428−446

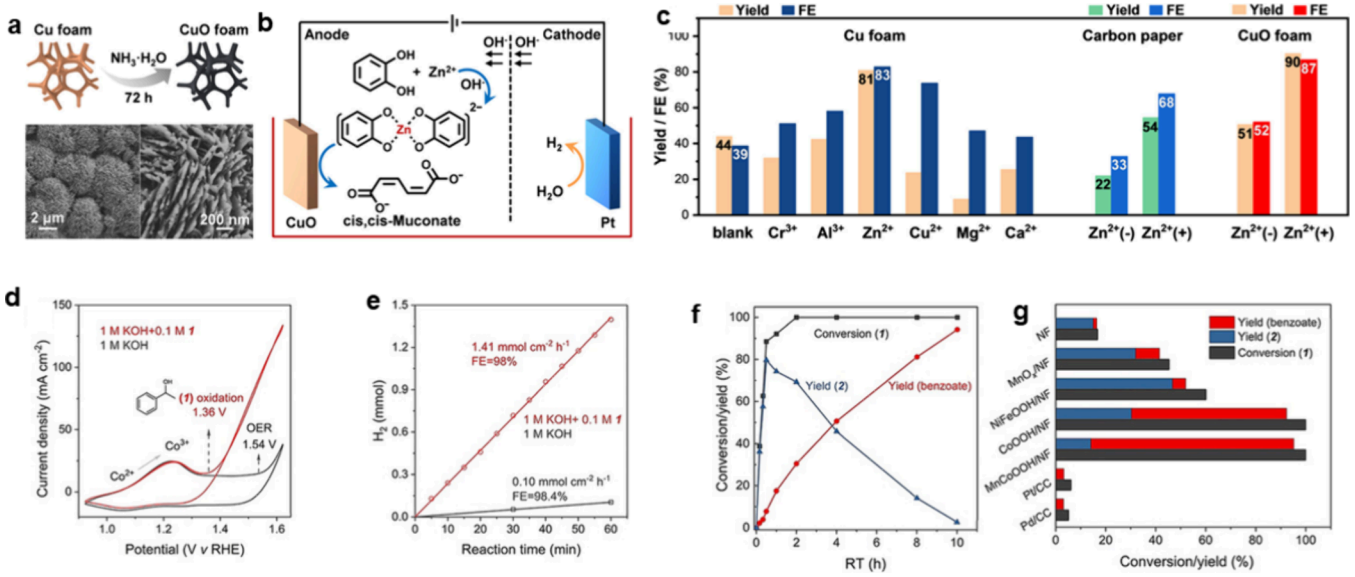

Figure 5. (a) Synthetic procedures of the CuO foam electrode and the scanning electron microscopy (SEM) images of the obtained CuO foam. (b) Schematic diagram of catechol electrooxidation at the anode and hydrogen production at the cathode. (c) Effects of different cations and different catalysts on the yield/FE of the catechol conversion to *cis*,*cis*-muconate. Reproduced from ref 28. Copyright 2023 American Chemical Society. (d) Cyclic voltammetric (CV) curves of MnCoOOH/nickel foam (NF) in 1 M KOH electrolyte with or without Phenethyl alcohol (**1**). (e) Cathodic H_2 evolution at 1.5 V vs reversible hydrogen electrode (RHE) in 1 M KOH with or without **1**. (f) Kinetic curves for the **1** transformation as a function of reaction time. Reaction conditions: 0.5 mmol of **1**, 50 mL of 1 M KOH, and MnCoOOH/NF(+)//Pt foil(−). (g) Comparison of the catalytic performances of other common catalysts and MnCoOOH/NF. Reaction conditions: 0.5 mmol **1**, 50 mL 1 M KOH, anodic catalyst(+)//Pt foil(−), 1.5 V vs RHE, 8 h. Reproduced from ref 32. Copyright 2021 John Wiley and Sons.

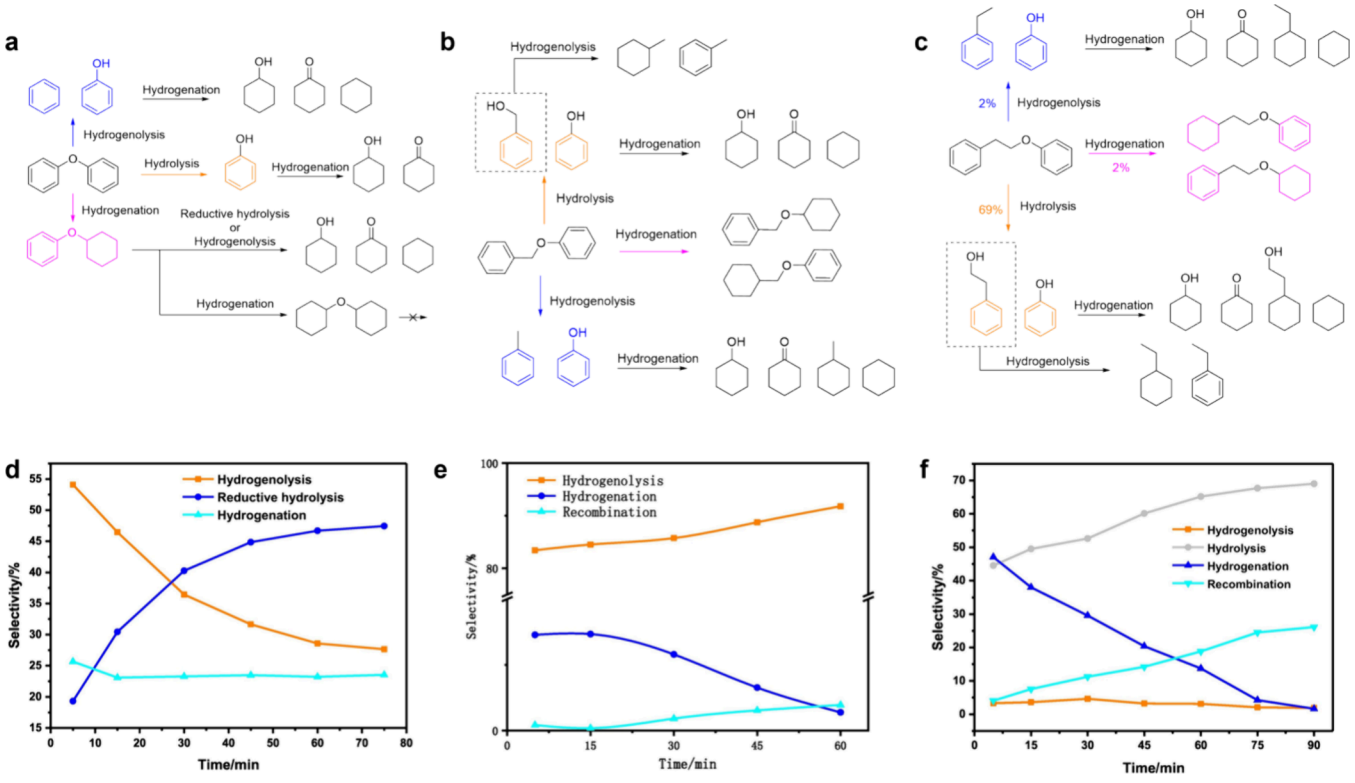

Figure 6. Value-added routes for reductive cleavage of lignin dimers (a) DPE, (b) BPE, and (c) PEB in the PW_{12}−Pt/C based ECH system. Product distribution for the conversion of (d) DPE, (e) BPE, and (f) PEB. Reaction conditions: 10 mM reactant; Pt to substrate, 5 mol %; PW_{12} (0.25 M); $NaBH_4$ (0.68 M); current density (25 mA cm^{-2}); temperature (80 °C). Reproduced from ref 51. Copyright 2022 Elsevier.

be categorized into two distinct mechanisms: reductive cleavage and oxidative cleavage.[50]

https://doi.org/10.1021/prechem.4c00024
Precis. Chem. 2024, 2, 428−446

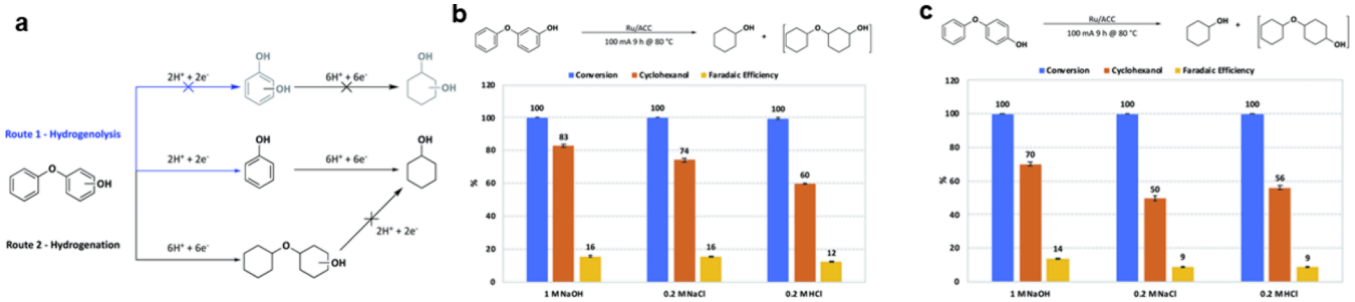

Figure 7. (a) Schematic reaction routes for the ECH of 3-phenoxyphenol and 4-phenoxyphenol. Observed products, conversion, cyclohexanol yield, and FE for ECH of 20 ± 4 mM 3-phenoxyphenol (b) and 4-phenoxyphenol (c) using 20 mL of the different electrolytes (1 M NaOH, 0.2 M HCl, 0.2 M NaCl) at 80 °C, 100 mA (33.3 mA cm^{-2}), for 9 h. Reproduced from ref 52. Copyright 2020 Royal Society of Chemistry.

3.1. Reductive Cleavage

Lignin dimers can undergo reductive cleavage through an ECH process to produce lignin monomers and their derivatives. Due to the difference in electronegativity between carbon and oxygen, the C−O bond can be polarized and undergo hydrogenolysis reaction at the cathode. Therefore, lignin dimers with 4-O-5, α-O-4, and β-O-4 linkages have the potential to undergo hydrogenolysis (Figure 6a−c).

The dual-catalyst suspension system has been demonstrated to exhibit impressive catalytic activity in the ECH of lignin monomers,[39] thus necessitating an investigation into its application in the reductive cleavage of lignin dimers. Xu et al. thoroughly investigated the product distributions of electroreduction for the 4-O-5 linkage (diphenyl ether (DPE)), α-O-4 linkage (benzyl phenyl ether (BPE)), and β-O-4 linkage (phenethoxybenzene (PEB)) in a phosphotungstic acid (PW_{12})-Pt/C based fluidized ECH system.[51] The turnover frequency (TOF) analysis of the different substrates revealed that the reaction rate of C−O bond cleavage decreased in the following order: α-O-4 > 4-O-5 > β-O-4. The analysis of the reaction products indicated that the C−O bond was predominantly cleaved through hydrogenolysis and hydrolysis. Notably, the hydrolysis reaction was not observed in open circuit conditions, indicating that the hydrolyzed products were formed through a reductive hydrolysis process, which necessitated the addition of H* followed by water attack. In addition, hydrogenation side reaction occurred on the phenyl group, resulting in precluding the cleavage of the C−O bond. The selectivity of the reaction pathways varied, depending on the specific reaction substrates.

The initial reaction of DPE primarily followed the pathway of hydrogenolysis. As the reaction progressed, the concentration of DPE decreased and the hydrolysis pathway became predominant (Figure 6d). For BPE, the analysis of the products revealed that the hydrogenolysis pathway was observed throughout the entire reductive cleavage process (Figure 6e). For PEB, during the initial stage of electroreduction, both hydrogenation and reductive hydrolysis pathways exhibited comparable selectivity (Figure 6f). However, as the concentration of PEB decreased, the selectivity of hydrogenation diminished, while hydrolysis became the predominant reaction pathway. Simultaneously, a recombination pathway emerged and was intensified. Moreover, the decrease in FE resulting from the HER could not be disregarded for all substrates. Although increasing the temperature could partially suppress HER, the FE of lignin dimer cleavage still remained below 55%.

Saffron and co-workers achieved electrocatalytic hydrogenolysis of 4-O-5 bonds in phenoxyphenol by a Ru loading onto an activated carbon cloth (ACC) catalyst, enabling direct production of KA oil from lignin dimers.[52] The ECH of both 3- and 4-phenoxyphenol was proposed to proceed through two pathways: one involves the cleavage of the 4-O-5 bond, resulting in the formation of phenol, which was subsequently hydrogenated to cyclohexanol (Figure 7a, route 1); the other pathway involved the hydrogenation of one or both aromatic rings without C−O bond cleavage (Figure 6, route 2). The hydroxyl group on the phenyl group was demonstrated to enhance substrate adsorption onto the catalyst surface, thereby augmenting the FE of hydrogenolysis. The optimal conditions for achieving the highest yield of cyclohexanol through hydrogenolysis involved an alkaline electrolyte, resulting in yields of 83% and 70% for 3- and 4-phenoxyphenol, respectively (Figure 7b, c). However, reductive cleavage of phenoxyphenol exhibited a significantly low FE (<16%), attributed to its strong C−O bond and limited reactivity.

The hydrogenolysis reaction pathway of α-O-4 and β-O-4 linkages on common catalysts (such as Pt/C, Ru/C, Rh/C, and Raney Ni) has been thoroughly investigated.[53,54] The results demonstrated that the cleavage products of lignin dimers were identified as phenol and corresponded to arene, respectively. Steric interactions caused by substituent groups on the aromatic groups could drastically diminish the efficiency of the reductive cleavage. The delocalization of C and O electrons in the phenyl group enhanced the reactivity of the C−O bond, leading to α-O-4 being more susceptible to cleavage compared to β-O-4. It is noteworthy that the hydrogenolysis of the C−O bond did not occur if the aromatics were hydrogenated first, which was attributed to the delocalization of electrons on the O atom being weakened by benzene hydrogenation, resulting in a more stable C−O bond that was challenging to be cleaved. Previous reports have demonstrated that reductive cleavage of the β-O-4 bond poses a greater challenge compared to that of the α-O-4 bond due to the lower polarity of the β-O-4 bond; however, the introduction of carbonyl groups on C_α can facilitate the cleavage efficiency. Stephenson and co-workers reported a potential-controlled electrolysis for the cleavage of lignin dimers with β-O-4 linkages in organic electrolyte.[55] The C−O bond of the lignin dimers with a C(O)−C−O linkage could be selectively cleaved at controlled potentials, leading to the formation of lignin monomers or coupling products with a yield ranging from 59% to 92%.

Overall, despite the comprehensive investigation on the cleavage selectivity of lignin dimers, the competition between ECH of the phenyl group and HER poses challenges to the development of more efficient reductive cleavage for lignin dimers.

https://doi.org/10.1021/prechem.4c00024
Precis. Chem. 2024, 2, 428−446

Scheme 4. Value-Added Products for Oxidative Cleavage of Lignin Dimers

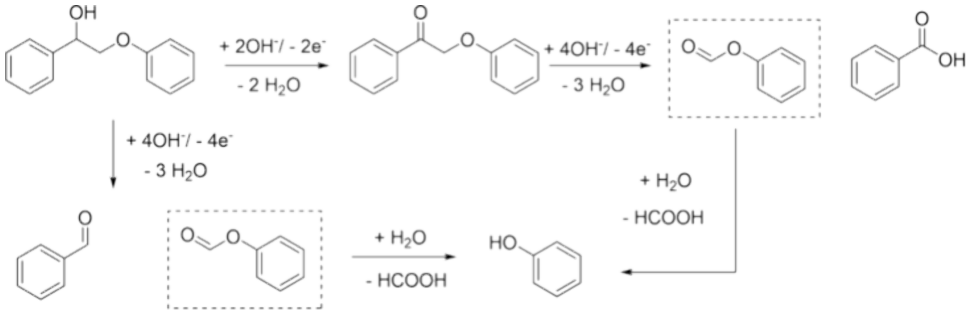

3.2. Oxidative Cleavage

The electrocatalytic oxidative cleavage of C−C or C−O bonds of biomass has been widely studied. For example, glycerol as a polyhydric alcohol could be converted to lactic acid, glycolic acid, and final formic acid by electrooxidation.[17] The C(O)−C bond of KA oil could be broken to generate adipic acid.[34,56] Furfural could be oxidatively reformed to maleic acid. Compared with the above organic compounds, lignin dimers possess the characteristics of an inert functional group and low solubility due to phenyl group. In terms of reaction mechanism, lignin dimers could be oxidatively cleavage through direct oxidation by reactive oxygen species or indirect oxidation by HAT mediators (Scheme 4).

3.2.1. Direct Oxidation by Reactive Oxygen Species.

Direct oxidation involves the charge transfer directly from organic compounds to the reactive oxygen species on electrocatalysts.[57] Specifically, there are adsorbed hydroxyl groups (OH*) or bridging oxygen species (μ_2-O) on the surface of catalysts generated under applied potentials. These electron-deficient species tend to grab the hydrogen atom of organic compounds by the PCET or PT−ET process. Subsequently, the C−C bonds of organic compounds adsorbed on the catalysts are directly cleaved. Li and co-workers evaluated the cleavage selectivity of β-O-4 linkage over Pt microdisc working electrode.[58] The hydroxy or carbonyl group on C_α of the β-O-4 linkage could induce C−C cleavage. Specifically, for 2-phenoxy-1-phenethanol, the phenolic group underwent an initial single electron transfer oxidation to form benzene radical cation. The HOMO of the benzene radical cation was delocalized over the phenolic group and β-O-4 linkage so that the β-O-4 linkage was activated. Therefore, the cleavage of C_α-C_β or C_β-O bonds in the cation intermediate of the lignin dimer would generate phenylacetaldehyde or benzaldehyde, respectively. For 2-phenoxyacetophenone, the enhanced electron delocalization ability of the carbonyl group, compared to that of the hydroxyl group on C_α in the β-O-4 linkage, led to a heightened propensity for the cleavage of C_α-C_β bonds. However, only C_β-O bond cleavage would take place in the process of the electrooxidation of 2-phenoxy-1-phenylethane to phenethyl alcohol and phenol. The presence of the C_α-hydroxyl group with induced delocalization of HOMOs was the key to cleaving C_α-C_β.

Ni-based catalysts exhibit remarkable reactivity in electrooxidation. Fleischmann proposed an "indirect oxidation mechanism", complemented by another mechanism called "potential-dependent oxidation" proposed by Choi.[59,60] For the above mechanism, there are three key similar steps: (1) reconstruction from $Ni(OH)_2$ to high-valence Ni active sites; (2) adsorption of organic compounds; and (3) reaction between organic compounds and high-valence Ni active sites (Scheme 5), despite the different real active Ni species and the rate determination step.

Scheme 5. Schematic Mechanism of (a) Indirect Oxidation and (b) Potential-Dependent Oxidation[a]

a

$$OH^- + Ni(OH)_2 \underset{\text{fast}}{\overset{-H^+,\,-e^-}{\rightleftharpoons}} NiOOH + H_2O \quad (1)$$

$$RCH_2OH_{sol} \rightleftharpoons RCH_2OH_{ads} \quad (2)$$

$$(RCH_2OH)_{ads} + NiOOH \xrightarrow{RDS} R\dot{C}HOH_{ads} + Ni(OH)_2 \quad (3)$$

$$R\dot{C}HOH_{ads} + 3NiOOH + H_2O \rightarrow\rightarrow RCOOH_{sol} + 3Ni(OH)_2 \quad (4)$$

b

$$2OH^- + Ni(OH)_2 \xrightarrow[-2H^+]{-2e^-} NiO_2 + 2H_2O \quad (1)$$

$$OH^- + RCH_2OH \rightleftharpoons RCH_2O^- + H_2O \quad (2)$$

$$RCH_2O^-_{sol} \rightleftharpoons RCH_2O^-_{ads} \quad (3)$$

$$RCH_2O^-_{ads} + NiO_2 \xrightarrow{\text{hydride transfer}} RCHO_{sol} + Ni(OH)O^- \quad (4)$$

$$Ni(OH)O^- + HO^- \xrightarrow[-H^+]{-2e^-} NiO_2 + H_2O \quad (5)$$

[a]Reproduced from ref 59. Copyright 2021 American Chemical Society.

Sun et al. realized the conversion of lignin pretreated by ethanol to vanillin and syringaldehyde by Ni foam directly.[63] NiOOH was demonstrated as the primary active species, initiating the oxidation of the hydroxy groups on C_α and subsequently cleaving the C_β−O bond in the β-O-4 linkage. The overall yield of the lignin monomer, however, was merely 18%.

Co-based electrocatalysts usually exhibit oxidative activity similar to that of Ni-based electrocatalysts, with lower onset potentials. Zhao and co-workers employed cobaltous sulfide (CoS) as an efficient anodic catalyst to establish a lignin battery and cleave the lignin at anode with the current density up to 100 mA cm^{-2}.[64] Similar to Ni-based catalysts, CoS underwent reconstruction to CoOOH with applied potentials, which were considered as real active sites for the cleavage of lignin. Although lignin is degraded mostly by cleavage of the β-O-4 bond, it is still hard to control the product selectivity of lignin degradation products. The side reaction products such as aliphatic acids from ring-opening reactions and CO_2 from mineralization reaction were observed. The recent progress in developing efficient electrocatalysts for oxidation cleavage of lignin dimers is shown in the "Heteroatom Doping" section.

Compared with oxidative cleavage mediated by direct oxidation, HAT-mediated oxidation often exhibits lower applied potentials and higher selectivity. HAT mediators such as *N*-hydroxyphthalimide (NHPI) or 2,2,6,6-tetramethylpiperidi-

https://doi.org/10.1021/prechem.4c00024
Precis. Chem. 2024, 2, 428−446

Scheme 6. Schematic of (a) NHPI-Mediated and (b) Mechanism of Alcohol Oxidation by Oxoammonium under Basic and Acidic Conditions; (c) ACT-Mediated Cleavage of Lignin Dimers[61a]

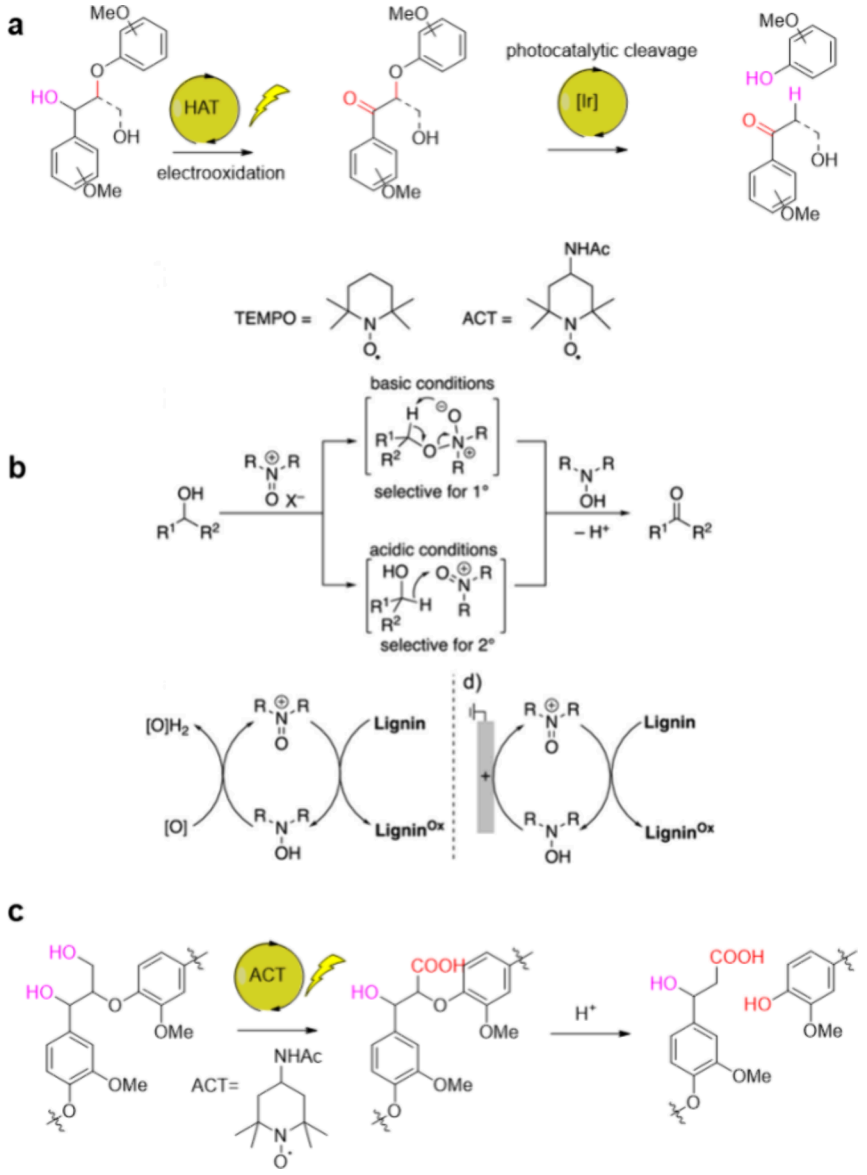

[a]Reproduced from ref 62. Copyright 2019 American Chemical Society.

nooxy (TEMPO) serve as redox intermediates in the oxidation of organic compounds.

3.2.2. HAT-Mediated Oxidation. For HAT-mediated oxidation, the mediators go through a two-step process including oxidation at the anode and the following reduction by organic compounds with reducibility.[65]

Stephenson's group reported a photocatalysis system by coupling NHPI/2,6-lutidine with iridium complex to achieve the cleavage of β-O-4 linkage.[61] In the neutral organic electrolyte system, NHPI would lose an electron to generate *N*-oxyl radicals, phthalimide *N*-oxyl (PINO). The effect of,6-lutidine was to make the PINO/NHPI redox couple more reversible. PINO, as an electron-deficient species, would oxidize the hydroxy group on C_α to carbonyl group and would be reduced back to NHPI, through which the lignin model compounds will be converted to secondary keto-products (Scheme 6a). The keto-products are subsequently cleaved by a photocatalytic process, a C−O cleavage method reported before.[66] Under acid or neutral conditions, the HAT-mediators will oxidize the hydroxy group via a bimolecular hydride transfer mechanism, which prefers to act on the secondary benzylic alcohol in lignin. Under alkaline conditions, the HAT-mediators tend to react with primary alcohol with less steric hindrance through an inner sphere mechanism (Scheme 6b).[62] Stahl and co-workers used a modified TEMPO, named 4-acetamido-TEMPO (ACT), to indirectly oxidize primary hydroxy groups to carboxyl groups in the β-O-4 linkage of lignin dimer in $NaHCO_3/Na_2CO_3$ electrolyte of pH = 10 (Scheme 6c).[62] The carboxyl intermediate had enhanced reactivity to be cleaved through the hydrolysis of the C_α-C_β bond. Moreover, this method enabled the cleavage of the C_α-C_β bond in the lignin dimer with an β-1 linkage.

Except for the recyclable HAT-mediators, our group reported a strategy through the addition of extra pt *tert*-butyl hydroperoxide (^{t}BuOOH), as a free radical initiator, to selectively cleave the β-O-4 linkage in a one-step way.[70] We demonstrated

https://doi.org/10.1021/prechem.4c00024
Precis. Chem. 2024, 2, 428−446

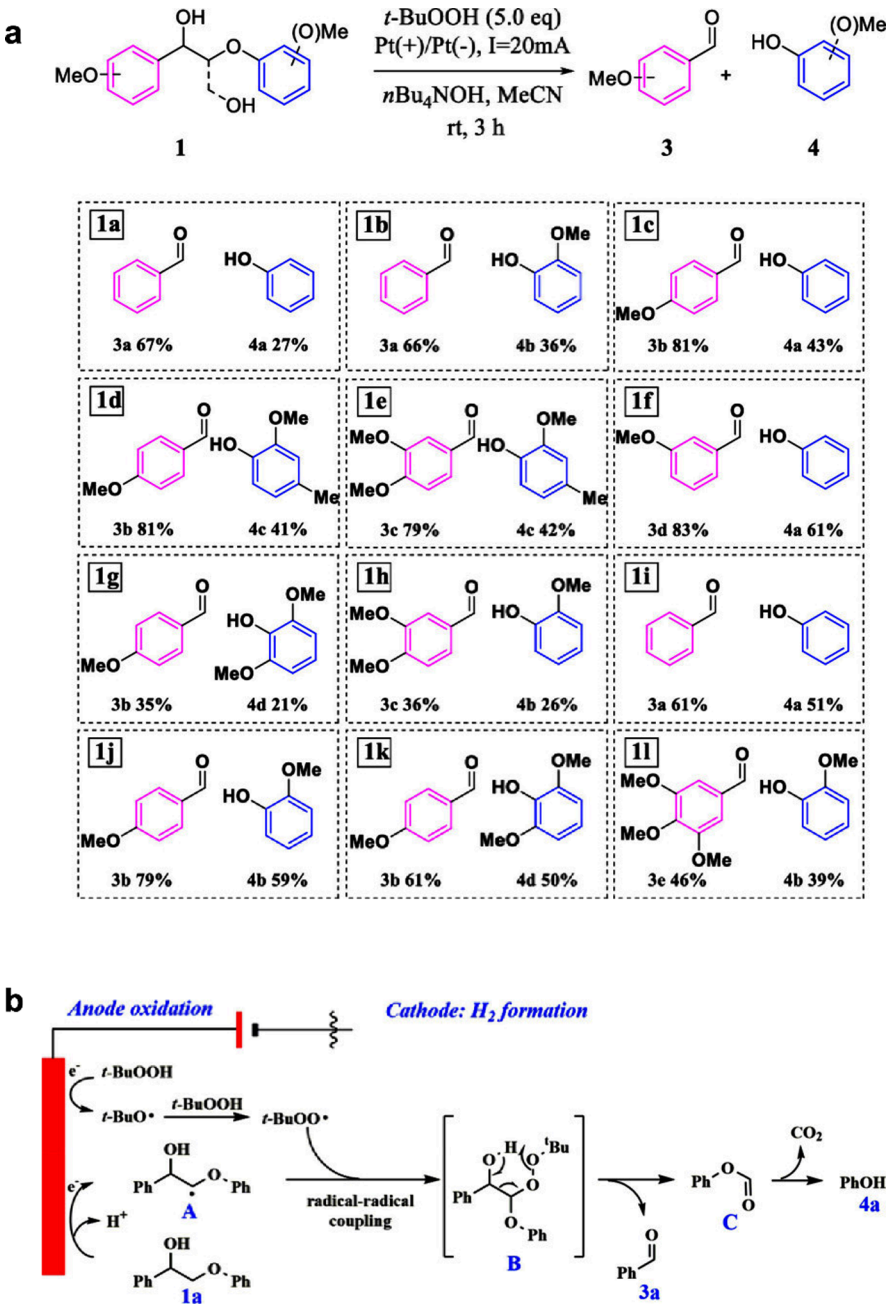

Figure 8. (a) Substrate scoping of the oxidative cleavage of typical lignin model compounds. Reaction conditions: substrate (0.2 mmol), *n*-Bu_4NOH (0.4 mmol), ^{t}BuOOH in water (70% aqueous solution) (1.0 mmol), MeCN (1.0 mL), room temperature, I = 20 mA, 3 h, under air. Compounds: **1i**–**1l**, lignin β-O-4 linkages with C_γ–OH; **3a**–**3l**, aromatic aldehyde products; **4a**–**4l**, phenol products. (b) Proposed mechanism for the electrocatalytic C_α–C_β bond cleavage of the β-O-4 lignin model compounds. Compounds: **A** secondary carbon radicals, **B** unstable intermediate, **C** phenyl formate. Reproduced from ref 61. Copyright 2021 American Chemical Society.

the excellent compatibility of this strategy toward oxidative cleavage of lignin dimers with diverse substituents on the phenol group (Figure 8a). Mechanism studies revealed that ^{t}BuOOH loses an electron to generate ^{t}BuO· free radicals on the surface of the Pt electrode. Simultaneously, the C_β atoms of lignin dimers with β-O-4 linkages underwent electron loss and transformed into secondary carbon radicals (**A**) (Figure 8b). The ^{t}BuO· and A radicals form an unstable intermediate (**B**) by C–O bond coupling. The intermediates underwent intramolecular electron transfer and C–C bond breakage to produce benzaldehyde (**3a**) and phenol (**4a**). The lignin dimer conversion and benzaldehyde yield achieved 93% and 67%, respectively.

4. RAW LIGNIN: EFFICIENT DEGRADATION

4.1. Degradation of Raw Lignin into Valuable Products

Based on the study about lignin monomer conversion and dimer cleavage, it is imperative to extend the investigations to electrocatalytic conversion of raw lignin with more complicated structures, considering practical significance. Li and co-workers thoroughly investigated the products of the oxidation of corn stover lignin catalyzed by PbO_2 anode coupled with cathodic ECH catalyzed by Cu/Ni–Mo–Co.[71] The degradation of raw lignin could yield plenty of valuable products, such as trans-ferulic acid, vanillin, 3-hydroxy-4-methoxyphenyl-ethanone,

https://doi.org/10.1021/prechem.4c00024
Precis. Chem. 2024, 2, 428–446

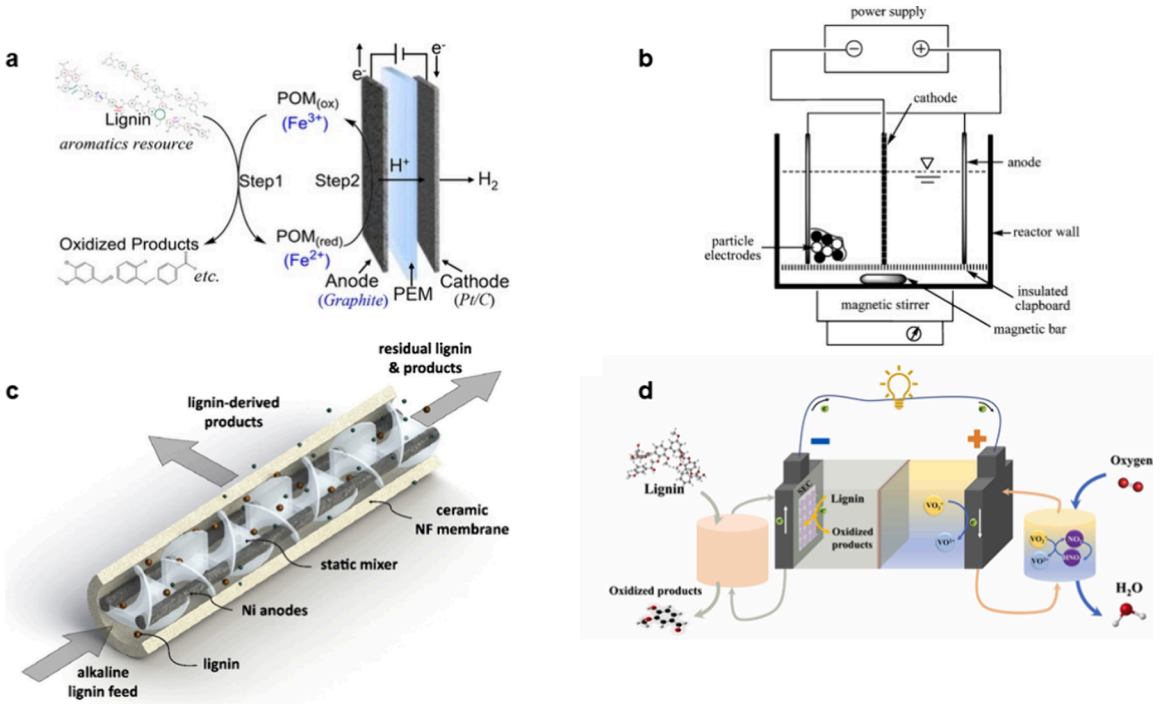

Figure 9. Schematic illustration of (a) hydrogen production system employing POM or $FeCl_3$ as a charge-transfer agent. Reproduced from ref 67. Copyright 2017 John Wiley and Sons. (b) TDE reactor with Pb/PbO_2 anode. Reproduced from ref 68. Copyright 2015 Elsevier. (c) electrochemical membrane reactor with an *in situ* nanoscale filtration. Reproduced from ref 69. Copyright 2015 Elsevier. (d) LFFC system powered by lignin oxidation. Reproduced from ref 64. Copyright 2023 Elsevier.

syringaldehyde, acetosyringone, and 4-methoxy-3-methyl-phenol, which were obtained in 22.40, 11.09, 2.37, 10.04, 6.95, and 38.83 g per kg of lignin, respectively. The commercially available Ni foam could be directly utilized as the working electrode for the oxidative degradation of raw lignin pretreated with ethanol.[63] Vanillin and syringaldehyde were identified as the primary small molecule products resulting from the degradation of sweetgum and aspen lignin, achieving a maximum yield of 17.5%.

The optimization of the reaction procedures is important for raw lignin degradation, aiming to minimize any side reactions and overall costs, thereby enhancing efficiency and economic viability. For instance, the dissolution of lignin and repolymerization of lignin monomers are pH-dependent, with alkaline conditions favoring recondensation/oligomerization or oxidative degradation of the monomers in a one-pot procedure.[62] To address this issue, a sequential degradation approach involving a preoxidation step followed by an acidifying hydrolysis step has been proposed. The primary hydroxyl group on C_γ of lignin was first oxidized to carboxyl group to form oxidized lignin with TEMPO to avoid overoxidation (Scheme 6b). The oxidized lignin was collected through an acidification-extraction process, followed by degradation at 100 °C by mixing it with H_2O/HCOOH in a ratio of 1:9. Consequently, the yield of monomeric aromatic products significantly increased from 5% in the one-pot procedure to 29% in the two-step procedure.

The degradation of lignin not only contributes to the production of value-added products but also enables further coupling with the cathodic reactions at counter electrode for added values. By substituting the degradation of lignin for the anodic oxygen evolution reaction (OER) during water electrolysis for hydrogen production, one could mitigate the overall cell voltage, thus decreasing energy consumption. Deng et al. introduced an indirect electrooxidation system employing POM or $FeCl_3$ as a charge-transfer agent, wherein raw lignin was utilized as the anodic hydrogen source to facilitate efficient hydrogen production (Figure 9a).[67] The conversion of lignin was realized through POM or Fe^{3+} by the similar two steps, including the oxidation of lignin by POM or Fe^{3+} in the electrolyte and the subsequent regeneration of POM or Fe^{3+}. The electric energy consumption was 2.54 $kWhNm^{-3}$ for POM and 2.30 $kWhNm^{-3}$ for $FeCl_3$, indicating a reduced electric energy of 39.5% (for POM) and 45.2% (for $FeCl_3$) compared to the previously reported best PEM water electrolysis (4.2 $kWhNm^{-3}$).[72]

The total values of products from raw lignin degradation can be also enhanced by coupling biomass reduction reactions at the cathode besides HER. The coupling strategy leads to a reduction in energy consumption as a result of the more favorable thermodynamics and/or kinetics associated with biomass reduction compared to HER. In this regard, Qin and co-workers developed an efficient bifunctional electrocatalyst by doping phosphorus (P) into $CoMoO_4$.[29] With a high raw lignin conversion rate (~100%) and the excellent selectivity of benzoic acid (56%) at the anode, the conversion of furfural (84%) and selectivity toward 2-methyl furan (78%) could be achieved in the ECH of furfural at the cathode, demonstrating the potential of coupling anodic and cathodic biomass conversion toward increasing the product economic values.

4.2. Design of Reactors for Raw Lignin Valorization

The design of reactors holds equal significance with the optimization of catalysts in the context of authentic lignin degradation. Li and co-workers developed a novel procedure in a three-dimensional electrode (TDE) reactor with Pb/PbO_2 anode for lignin degradation.[73] The TDE reactor was mainly made of an undivided-volume cylindrical glass tank (Figure 9b).

https://doi.org/10.1021/prechem.4c00024
Precis. Chem. 2024, 2, 428−446

Granular activated carbon (GAC) electrode was filled between the PbO_2/Pb anode and stainless steel wire mesh cathode, which were suspended in the glass tank. A microporous plate was placed at the bottom of electrode to support the particle electrode to form a three-dimensional electrode. Sodium hydroxide (1 mol L^{-1}) solution dissolving 40 g L^{-1} aspen lignin was filled in the TDE reactor. When the degradation process ended after 8 h electrolysis under optimized conditions, the concentration of the main product, 4-methylanisole, reached 343.3 (g kg^{-1} lignin). The TDE reactor introduces particle electrode materials such as GAC to form charged microelectrodes and increase the specific surface areas in contact with the lignin. Thus, the performance of lignin degradation is improved by the enhanced mass transfer or the adsorption of lignin through this strategy.

The flow cell exhibits a significant enhancement in the mass transfer of lignin and thereby enhances the degradation efficiency compared to conventional devices (Figure 9c). An electrochemical membrane reactor for the continuous electrochemical cleavage of lignin integrated with an in situ nanoscale filtration process was designed to orthotopically remove the degradation products from lignin selectively.[69] Specifically, the cleavage of lignin took place inside the tubular ceramic membrane catalyzed by Ni rods when the low-molecular-weight degradation products were directly separated from the electrolyte by a slight overpressure on the anode side. A helical static mixer runs through the Ni rods in the tubular device to enhance the mass transfer of lignin. The tubular nanofiltration membrane coated in a poly(methyl methacrylate) (PMMA) tube was used to diffuse the low-molecular-weight molecules and retain the high-molecular-weight lignin. In the cathode chamber, a Ni felt with porosity placed in another PMMA tube was used as a counter electrode. An anion exchange membrane (AEM) was positioned between the cathode chamber and the anode chamber to separate them. Through the designed electrochemical membrane reactor, the production rate was more than doubled and the effects of fouling phenomena over the membrane were successfully removed. Besides, the products could be separated in situ from the lignin electrolyte without downstream processing.

In addition to the utilization of electrolytic devices for lignin degradation, raw lignin can also be harnessed in fuel cells for direct electricity generation. Zhao et al. designed a liquid flow fuel cell (LFFC) system, powered by lignin oxidation, which can generate electricity and simultaneously produce valuable lignin monomers (Figure 9d).[64] Using the vanadium(V) acyl ion (VO_2^+)/vanadium(IV) acyl ion (VO^{2+}) redox couple in the cathode chamber, the highest peak power density reached 176 mW cm^{-2} at 80 °C. The reduced VO^{2+} at the cathode could be oxidized back to VO_2^+ by HNO_3 to realize the circulation. Although the LFFC technology demonstrated a high efficiency in lignin-to-electricity conversion, the lack of selectivity in lignin products poses challenges for their separation.

5. DESIGN OF ELECTROCATALYSTS FOR LIGNIN VALORIZATION

The rational design of electrocatalysts in electrocatalytic conversion of lignin (expanding from monomers to dimers and finally to raw lignin) plays a pivotal role in promoting activity, selectivity, and FE. Therefore, it is necessary to summarize the recent advancement of catalyst design for lignin electrocatalysis. Three primary strategies including modulation of the metal−support interaction, heteroatom doping, and nanostructure construction have been developed, all of which are based on the electronic or stereochemical structure regulation of the active center. The electrocatalytic performance of lignin valorization could also be modulated by employing multidisciplinary strategies.

5.1. Metal−Support Interaction

The modulation of the metal−support interaction can effectively regulate the electronic structure of the metal active center, thereby influencing the adsorption energy of organics on the active sites.

Alternative carbon supports can be employed for the modification of the metal substrate. The ECH reactivity for lignin monomers could be enhanced by the addition of Ru loading on ACC.[75] Shrimp shell biochar (SSB) with high nitrogen served as a carrier for the Pt electrocatalyst, exhibiting exceptional stability and achieving complete conversion of phenol with a total selectivity of 98% toward cyclohexanone and cyclohexanol (Table 1).[74] Through the correlated analysis and

Table 1. Electrocatalytic Performance of ECH of Phenol with Different Metal Catalysts

Catalyst	Reactant	Selectivity of cyclohexanone (%)	Total FE (%)	Reference
Pt/XC-72R	phenol	66%	72	35
Pt/SSB	phenol	65.0%	78.1%	74
Ru/ACC	phenol	1.0%	29.0%	75
Ru/TiO_2	phenol	<1.0%	34.6%	76
Ni_{10}@ MoO_2/C	phenol	5%	98%	27
Ni_{20}@ MoO_2/C	phenol	86%	98%	27

DFT calculations, the significant roles C−O, Pt, and Pt−N_x sites played in phenol conversion were identified. Transition-metal oxides are extensively employed as supports of precious metals in various applications. Ru was loaded onto three-dimensional titanium dioxide (TiO_2) nanorods possessing abundant active sites and extensive microflow channels, enabling the preparation of a highly efficient catalyst for the phenol ECH process.[76] The reduction of cyclohexanone intermediates to cyclohexanol was further accelerated, resulting in a remarkable selectivity of over 99% for cyclohexanol. The product selectivity of phenol ECH was effectively regulated by controlling the O_V content on the MoO_2 support.[27]

The Ni_{10}@MoO_2/C catalyst exhibited a higher density of O_V, thereby facilitating adsorption of the cyclohexanone intermediate and promoting its excessive hydrogenation, resulting in a remarkable selectivity of 95% toward cyclohexanol. Conversely, the increased content of Ni over Ni_{20}@MoO_2/C reduced the density of oxygen vacancies, leading to enhanced desorption of cyclohexanone and thus achieving a selectivity of 86% toward cyclohexanone.

5.2. Heteroatom Doping

Heteroatom doping is a widely adopted strategy for catalyst design that exhibits the capability to regulate the electronic structures of active sites with promoted activity and selectivity by tuning the adsorption energy of reactants and/or reaction intermediates.

The doping of a third element into bimetallic alloys has been reported to highly promote lignin monomer conversion. For instance, the electronic structure of PtNi was modified through boron (B) alloying, delivering a mixture of KA oil with 90% FE

https://doi.org/10.1021/prechem.4c00024
Precis. Chem. 2024, 2, 428−446

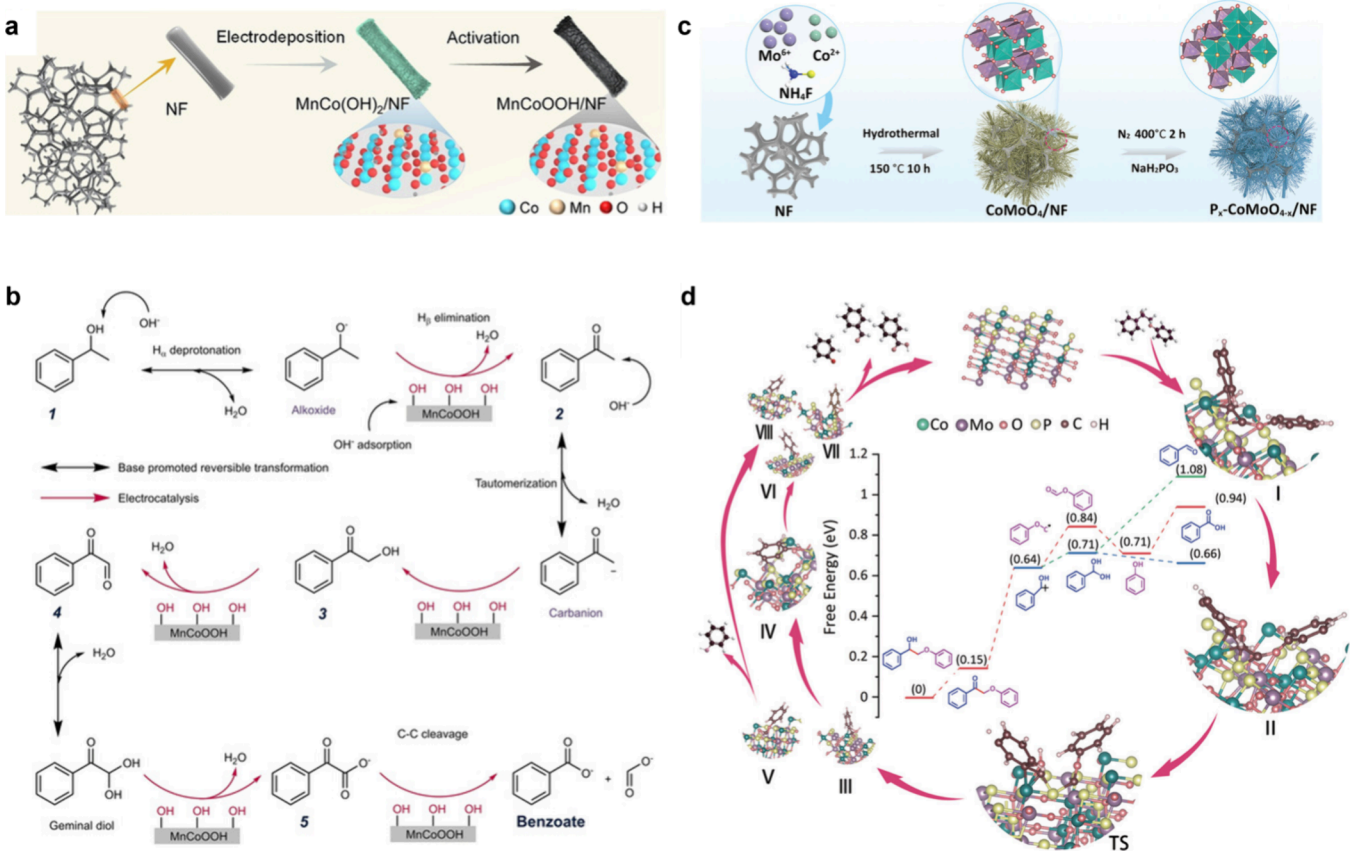

Figure 10. (a) Schematic illustration of the synthesis of MnCoOOH/NF. (b) Schematic mechanism of the C_α-C_β cleavage of acetophenone over MnCoOOH. Compounds: **1** Phenethyl alcohol, **2** acetophenone, **3** 2-hydroxyacetophenone, **4** 2-oxo-2-phenylacetaldehyde, **5** benzoylformic acid. Reproduced from ref 32. Copyright 2021 John Wiley and Sons. (c) Schematic illustration of the synthesis of P_x-$CoMoO_{4-x}$/NF. (d) DFT result for 2-phenoxy-1-phenethanol over P-doped $CoMoO_4$. Reproduced from ref 29. Copyright 2023 John Wiley and Sons.

and a conversion rate of 97.5%. Moreover, the selectivity of cyclohexanol could reach 89.8%.[77] Notably, the doping of B significantly influenced the adsorption energy of reaction intermediates on the surface of PtNiB, thereby enhancing the FE. Wang et al. reported that the PtRh bimetallic alloy exhibited high activity as an ECH catalyst.[78] Sargent, Zhao, and co-workers further synthesized a PtRhAu ternary alloy catalyst by incorporating Au into the PtRh catalyst. The PtRhAu catalyst exhibited a high FE of 58% and a high partial current density of 116 mA cm^{-2} toward the 2-methoxycyclohexanol from ECH of guaiacol.[43] The modulation of Pt catalysts with Rh and Au on PtRhAu catalysts could enhance guaiacol coverage, promote hydrogenation, and suppress demethoxylation. In another case, a trimetallic Pt3RuSn catalyst exhibited exceptional catalytic performance due to the incorporation of Sn into the Pt3Ru alloy, which provided new adsorption sites at the interface and significantly enhanced the conversion of cyclohexanone to cyclohexanol.[79]

The heteroatom doping strategy is not limited to metallic alloys but is successfully applied in metallic oxides and oxyhydroxides. Our group recently reported MnCoOOH to catalyze cleavage of the C_α−C_β bond in a lignin dimer with a β-O-4 linkage (Figure 10a).[32] **1** was used as the model compound to study the electrocatalytic performance of MnCoOOH. Then the substrate scope was extended to a series of lignin dimers with a C_α−C_β bond. Mechanism study indicated that 1 first underwent deproteination and H_β elimination to generate acetophenone (**2**) (Figure 10b). Then, **2** went through a tautomerization process and was hydroxylated to form 2-hydroxy-1-phenylacetone (**3**) which was identified as an RDS by DFT calculations. OH* was demonstrated as the main electrophilic oxygen species on the surface of MnCoOOH. During the reaction, the doped Mn would be transformed to a high-valence state with an unpaired $3d^3$ electron configuration. The property of electron deficiency on Mn would extract local electrons from Co sites, which could enhance the adsorption of OH^- and reduce the adsorption free energy of OH* to promote cleavage of the C(OH)−C or C(O)−C bond.

P could be also employed as the doping element into $CoMoO_4$ to achieve high conversion in the degradation of the lignin model compounds (Figure 10c).[29] In the Co 2p XPS spectra, doped P induced a peak shift to higher binding energy. After P doping, the intensity of Mo^{6+} significantly decreased and relatively low-valence Mo species such as Mo^{5+} and Mo^{4+} appeared in Mo 2p XPS spectra. O 1s XPS results showed increased contents of oxygen vacancies. The above results revealed that P doping promoted the internal electron transfer and generation of oxygen vacancies. Mo and Co sites with strong oxyphilic properties because of their high positive charge and unfilled d orbitals could promote the adsorption of β-O-4 type lignin dimers. In situ infrared spectroscopies and DFT calculations revealed that the incorporation of P enhanced the antibonding orbital energy level and promoted the adsorption of C_α−C_β bonds of lignin model substrates (Figure 10d). Therefore, the conversion of lignin dimers is obviously promoted over P-$CoMoO_4$ compared to that of $CoMoO_4$.

https://doi.org/10.1021/prechem.4c00024
Precis. Chem. 2024, 2, 428−446

5.3. Nanostructuring

Design of catalysts with unique nanostructures by morphology and size control is also efficient to enhance catalytic performance for electrocatalytic lignin conversion. Our group collaborated with Wang et al. and recently synthesized a single-atom Pt dispersed on nitrogen-doped carbon nanotubes named Pt_1/N-CNTs as an electrocatalyst for selective $C_\alpha-C_\beta$ bond oxidative cleavage in lignin dimers (Figure 11a).[80] The reaction

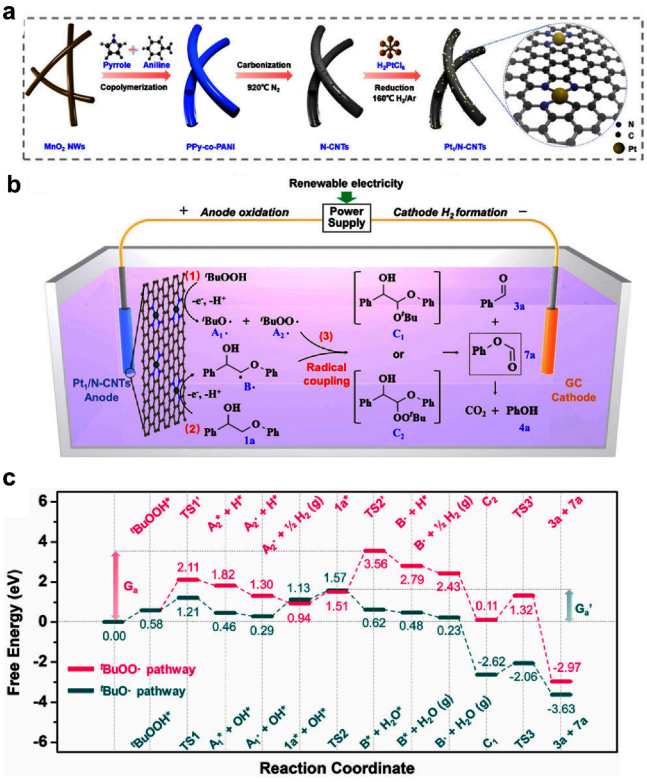

Figure 11. Synthetic strategy of the Pt_1/N-CNTs catalyst and reaction pathway based on experiments and DFT calculations. (a) Schematic illustration of the preparation of Pt_1/N-CNTs. (b) Proposed mechanism of Pt_1/N-CNTs-catalyzed conversion of 1a. Compounds: $\mathbf{A_1}$· *tert*-butoxyl radical (^{t}BuO·), $\mathbf{A_2}$· *tert*-butyl peroxyl radical (^{t}BuOO·), **B**· C_β radical, $\mathbf{C_1}$, $\mathbf{C_2}$, coupling intermediate, **1a** 2-phenoxy-1-phenylethanol, **3a** benzaldehyde, **4a** phenol, **7a** phenyl formate. (c) DFT-calculated potential energy surface for 1a conversion on the Pt_1/N-CNTs surface. Reproduced from ref 80. Copyright 2021 American Chemical Society.

mechanism is similar to that reported in our previous work.[70] ^{t}BuOOH and lignin dimer lost one electron and one proton, respectively, on the surface of Pt_1/N-CNTs to form an oxyalcohol radical (**A1**· or **A2**·) and secondary C_β radical (**B**·) (Figure 11b). The unstable intermediate (**C1** or **C2**) was formed by coupling **A1**· or **A2**· with **B**·, followed by intramolecular electron transfer to yield benzaldehyde (**3a**) and phenyl oxymethyl ether (**7a**). The hydrolyzation of the latter can form phenol. The high performance was demonstrated by comparison with nanosize Pt and Pt foil. The catalytic results indicated that the Pt_1/N-CNTs showed advantages over all other catalysts for both conversion and selectivity of the benzaldehyde product. The Pt L_3-edge X-ray absorption spectra demonstrated the Pt existed as single atoms, and the corresponding fitting analysis revealed that the active unit was $Pt-N_3C_1$, in which one Pt atom was coordinated with one C atom and three N atoms. DFT calculations revealed that the key step during lignin dimer degradation was the generation of the C_β radical (Figure 11c), which was facilitated by Pt_1/N-CNTs, thus promoting $C_\alpha-C_\beta$ bond cleavage. At an extremely low Pt loading of 0.41 wt %, high conversion of lignin dimer (99%) could be achieved with the yield of benzaldehyde reaching 81%.

6. CONCLUSIONS AND PERSPECTIVES

In this Review, we summarize the progress in electrocatalytic lignin refinery, including the valorization of lignin monomers, the cleavage of lignin dimers, and the degradation of raw lignin. At last, the rational design of catalysts is discussed. Despite significant advances, the fundamental and application aspects of electrocatalytic lignin valorization still face many challenges.

First, although many advanced electrocatalysts were synthesized for electrocatalytic lignin conversion, the FE and product selectivity required substantial improvements. For example, for electrochemical reduction, although noble-metal-based catalysts, such as Pt, Rh, Pd, and Ru, are favorable for electrochemical reduction, their high activity for the competitive reaction, HER, will diminish the FE and energy efficiency. For electrochemical oxidation, although Ni- and Co-based catalysts or HAT mediators exhibit high activity, further enhancement of the productivity and selectivity toward the desired products is necessary. Several strategies, including metal−support interactions, heteroatom doping, and nanostructuring, have yielded promising preliminary results and may guide the future direction of catalyst design. Moreover, the advancement of characterization techniques enables a more precise elucidation of the reaction mechanism. Different ex situ, in situ, and more importantly operando characterization techniques from different aspects can facilitate the probing of reaction intermediates and identification of the authentic reactive sites, with comprehensive understanding of the reaction mechanism, which would greatly help the rational design of more effici ent catalysts and reaction systems for electricity-driven lignin conversion.[28,30]

Second, the majority of systems focus on the conversion of lignin model compounds. The investigation of raw lignin valorization should be strengthened. The integration of catalyst design and the flow-cell system represent the forefront in enhancing the productivity and selectivity of raw lignin conversion. Alternatively, the integration of electrocatalysis and other multiple catalytic approaches was demonstrated as a promising research direction. For instance, a recent study demonstrated the successful achievement of highly selective lignin conversion using compartmented photo-electro-biochemical cells.[81] By comprehensively designing the electrochemical devices, there is potential to meet the industrial demands for electrochemical refinery of raw lignin.

Last but not least, the design of coupling reaction systems to make use of both an anode and a cathode for biomass valorization is worth in-depth exploration. The characteristic of electrocatalysis lies in the simultaneous occurrence of oxidation and reduction at the anode and the cathode, respectively. Thus, maximizing electron utilization by biomass conversion at both electrodes is attractive. The lignin can be electrocatalytically degraded at the anode, while the reduction reaction of biomass takes place at the cathode to lower the cell voltages and enhance the product values.[29] Similarly, the coupling of the simultaneous reduction of phenol to cyclohexanol at the cathode and the oxidation of phenol to benzoquinone at the anode was realized.[28] There are still

https://doi.org/10.1021/prechem.4c00024
Precis. Chem. 2024, 2, 428−446

many opportunities for us to explore, such as the design of more delicate coupling systems for biomass valorization with enhanced activity, selectivity, and product values.

AUTHOR INFORMATION

Corresponding Author

Haohong Duan − *Department of Chemistry, Tsinghua University, Beijing 100084, China; Haihe Laboratory of Sustainable Chemical Transformations, Tianjin 300192, China; Engineering Research Center of Advanced Rare Earth Materials, (Ministry of Education), Department of Chemistry, Tsinghua University, Beijing 100084, China;* orcid.org/0000-0002-9241-0984; Email: hhduan@mail.tsinghua.edu.cn

Authors

Xiang Liu − *Department of Chemistry, Tsinghua University, Beijing 100084, China*

Ye Wang − *Department of Chemistry, Tsinghua University, Beijing 100084, China*

Complete contact information is available at: https://pubs.acs.org/10.1021/prechem.4c00024

Author Contributions

All authors have given approval to the final version of the manuscript.

Notes

The authors declare no competing financial interest.

ACKNOWLEDGMENTS

This work was supported by the National Key R&D Program of China (2023YFA1507400), the Haihe Laboratory of Sustainable Chemical Transformations, the National Natural Science Foundation of China (Grant No. 22325805, 21935001), Beijing Natural Science Foundation (JQ22003).

REFERENCES

(1) Jing, Y.; Guo, Y.; Xia, Q.; Liu, X.; Wang, Y. Catalytic Production of Value-Added Chemicals and Liquid Fuels from Lignocellulosic Biomass. *Chem.* **2019**, *5* (10), 2520−2546.

(2) Ragauskas, A. J.; Beckham, G. T.; Biddy, M. J.; Chandra, R.; Chen, F.; Davis, M. F.; Davison, B. H.; Dixon, R. A.; Gilna, P.; Keller, M.; Langan, P.; Naskar, A. K.; Saddler, J. N.; Tschaplinski, T. J.; Tuskan, G. A.; Wyman, C. E. Lignin Valorization: Improving Lignin Processing in the Biorefinery. *Science* **2014**, *344* (6185), 1246843.

(3) Sun, Z.; Fridrich, B.; de Santi, A.; Elangovan, S.; Barta, K. Bright Side of Lignin Depolymerization: Toward New Platform Chemicals. *Chem. Rev.* **2018**, *118* (2), 614−678.

(4) Theerathanagorn, T.; Kessaratikoon, T.; Rehman, H. U.; D'Elia, V.; Crespy, D. Polyhydroxyurethanes from Biobased Monomers and CO2: A Bridge between Sustainable Chemistry and CO2 Utilization†. *Chin. J. Chem.* **2024**, *42* (6), 652−685.

(5) Wang, Z. Y.; Sun, Y.; Sun, G. D.; Xu, H.; Dai, H. X. Total Synthesis of Syringin and Its Natural Analogues via C—C Bond Activation of Aryl Ketones†. *Chin. J. Chem.* **2023**, *41* (24), 3587−3592.

(6) Stone, M. L.; Webber, M. S.; Mounfield, W. P.; Bell, D. C.; Christensen, E.; Morais, A. R. C.; Li, Y.; Anderson, E. M.; Heyne, J. S.; Beckham, G. T.; Román-Leshkov, Y. Continuous hydrodeoxygenation of lignin to jet-range aromatic hydrocarbons. *Joule* **2022**, *6* (10), 2324−2337.

(7) Yang, X.; Zhang, P.; Zhou, Y.; Wang, J.; Liu, H. Synthesis and Antioxidant Activities of Novel 4,4′-Arylmethylene-bis(1H-pyrazole-5-ol)s from Lignin. *Chin. J. Chem.* **2012**, *30* (3), 670−674.

(8) Dong, L.; Lin, L.; Han, X.; Si, X.; Liu, X.; Guo, Y.; Lu, F.; Rudić, S.; Parker, S. F.; Yang, S.; Wang, Y. Breaking the Limit of Lignin Monomer Production via Cleavage of Interunit Carbon-Carbon Linkages. *Chem.* **2019**, *5* (6), 1521−1536.

(9) Shao, Y.; Xia, Q.; Dong, L.; Liu, X.; Han, X.; Parker, S. F.; Cheng, Y.; Daemen, L. L.; Ramirez-Cuesta, A. J.; Yang, S.; Wang, Y. Selective production of arenes via direct lignin upgrading over a niobium-based catalyst. *Nat. Commun.* **2017**, *8* (1), 16104.

(10) Xia, Q.; Chen, Z.; Shao, Y.; Gong, X.; Wang, H.; Liu, X.; Parker, S. F.; Han, X.; Yang, S.; Wang, Y. Direct hydrodeoxygenation of raw woody biomass into liquid alkanes. *Nat. Commun.* **2016**, *7* (1), 11162.

(11) Li, H.; Bunrit, A.; Lu, J.; Gao, Z.; Luo, N.; Liu, H.; Wang, F. Photocatalytic Cleavage of Aryl Ether in Modified Lignin to Non-phenolic Aromatics. *ACS Catal.* **2019**, *9* (9), 8843−8851.

(12) Liu, H.; Li, H.; Luo, N.; Wang, F. Visible-Light-Induced Oxidative Lignin C-C Bond Cleavage to Aldehydes Using Vanadium Catalysts. *ACS Catal.* **2020**, *10* (1), 632−643.

(13) Luo, N.; Wang, M.; Li, H.; Zhang, J.; Hou, T.; Chen, H.; Zhang, X.; Lu, J.; Wang, F. Visible-Light-Driven Self-Hydrogen Transfer Hydrogenolysis of Lignin Models and Extracts into Phenolic Products. *ACS Catal.* **2017**, *7* (7), 4571−4580.

(14) Luo, N.; Wang, M.; Li, H.; Zhang, J.; Liu, H.; Wang, F. Photocatalytic Oxidation-Hydrogenolysis of Lignin β-O-4 Models via a Dual Light Wavelength Switching Strategy. *ACS Catal.* **2016**, *6* (11), 7716−7721.

(15) Hilgers, R.; van Dam, A.; Zuilhof, H.; Vincken, J.-P.; Kabel, M. A. Controlling the Competition: Boosting Laccase/HBT-Catalyzed Cleavage of a β-O-4′ Linked Lignin Model. *ACS Catal.* **2020**, *10* (15), 8650−8659.

(16) Cai, C.; Xu, Z.; Zhou, H.; Chen, S.; Jin, M. Valorization of lignin components into gallate by integrated biological hydroxylation, O-demethylation, and aryl side-chain oxidation. *Sci. Adv.* **2021**, *7* (36), No. eabg4585.

(17) Wu, J.; Liu, X.; Hao, Y.; Wang, S.; Wang, R.; Du, W.; Cha, S.; Ma, X. Y.; Yang, X.; Gong, M. Ligand Hybridization for Electro-reforming Waste Glycerol into Isolable Oxalate and Hydrogen. *Angew. Chem., Int. Ed.* **2023**, *62* (9), No. e202216083.

(18) Zhou, B.; Li, Y.; Zou, Y.; Chen, W.; Zhou, W.; Song, M.; Wu, Y.; Lu, Y.; Liu, J.; Wang, Y.; Wang, S. Platinum Modulates Redox Properties and 5-Hydroxymethylfurfural Adsorption Kinetics of Ni(OH)(2) for Biomass Upgrading. *Angew. Chem., Int. Ed.* **2021**, *60* (42), 22908−22914.

(19) Ji, K.; Xu, M.; Xu, S. M.; Wang, Y.; Ge, R.; Hu, X.; Sun, X.; Duan, H. Electrocatalytic Hydrogenation of 5-Hydroxymethylfurfural Promoted by a Ru1Cu Single-Atom Alloy Catalyst. *Angew. Chem., Int. Ed.* **2022**, *61* (37), No. e202209849.

(20) Ge, R.; Wang, Y.; Li, Z.; Xu, M.; Xu, S. M.; Zhou, H.; Ji, K.; Chen, F.; Zhou, J.; Duan, H. Selective Electrooxidation of Biomass-Derived Alcohols to Aldehydes in a Neutral Medium: Promoted Water Dissociation over a Nickel-Oxide-Supported Ruthenium Single-Atom Catalyst. *Angew. Chem., Int. Ed.* **2022**, *61* (19), No. e202200211.

(21) Sheng, H.; Janes, A. N.; Ross, R. D.; Hofstetter, H.; Lee, K.; Schmidt, J. R.; Jin, S. Linear paired electrochemical valorization of glycerol enabled by the electro-Fenton process using a stable NiSe2 cathode. *Nat. Catal.* **2022**, *5* (8), 716−725.

(22) Gao, Y.; Ge, L.; Xu, H.; Davey, K.; Zheng, Y.; Qiao, S.-Z. Electrocatalytic Refinery of Biomass-Based 5-Hydroxymethylfurfural to Fine Chemicals. *ACS Catal.* **2023**, *13* (17), 11204−11231.

(23) Chen, C.; Jin, H.; Wang, P.; Sun, X.; Jaroniec, M.; Zheng, Y.; Qiao, S. Z. Local reaction environment in electrocatalysis. *Chem. Soc. Rev.* **2024**, *53* (4), 2022−2055.

(24) Yang, C.; Maldonado, S.; Stephenson, C. R. J. Electrocatalytic Lignin Oxidation. *ACS Catal.* **2021**, *11* (16), 10104−10114.

(25) Wijaya, Y. P.; Smith, K. J.; Kim, C. S.; Gyenge, E. L. Electrocatalytic hydrogenation and depolymerization pathways for lignin valorization: toward mild synthesis of chemicals and fuels from biomass. *Green Chem.* **2020**, *22* (21), 7233−7264.

(26) Garedew, M.; Lam, C. H.; Petitjean, L.; Huang, S.; Song, B.; Lin, F.; Jackson, J. E.; Saffron, C. M.; Anastas, P. T. Electrochemical

upgrading of depolymerized lignin: a review of model compound studies. *Green Chem.* **2021**, *23* (8), 2868−2899.
(27) Zhou, P.; Guo, S. X.; Li, L.; Ueda, T.; Nishiwaki, Y.; Huang, L.; Zhang, Z.; Zhang, J. Selective Electrochemical Hydrogenation of Phenol with Earth-abundant Ni-MoO2 Heterostructured Catalysts: Effect of Oxygen Vacancy on Product Selectivity. *Angew. Chem., Int. Ed.* **2023**, *62* (8), No. e202214881.
(28) Wang, R.; Li, C.; Wu, J.; Du, W.; Jiang, T.; Yang, Y.; Yang, X.; Gong, M. Coordination-Promoted Bio-Catechol Electro-Reforming toward Sustainable Polymer Production. *J. Am. Chem. Soc.* **2023**, *145* (33), 18516−18528.
(29) Qi, Y.; Liu, B.; Qiu, X.; Zeng, X.; Luo, Z.; Wu, W.; Liu, Y.; Chen, L.; Zu, X.; Dong, H.; Lin, X.; Qin, Y. Simultaneous Oxidative Cleavage of Lignin and Reduction of Furfural via Efficient Electrocatalysis by P-Doped CoMoO4. *Adv. Mater.* **2023**, *35* (14), No. e2208284.
(30) Peng, T.; Zhang, W.; Liang, B.; Lian, G.; Zhang, Y.; Zhao, W. Electrocatalytic valorization of lignocellulose-derived aromatics at industrial-scale current densities. *Nat. Commun.* **2023**, *14* (1), 7229.
(31) Wu, R.; Meng, Q.; Yan, J.; Liu, H.; Zhu, Q.; Zheng, L.; Zhang, J.; Han, B. Electrochemical Strategy for the Simultaneous Production of Cyclohexanone and Benzoquinone by the Reaction of Phenol and Water. *J. Am. Chem. Soc.* **2022**, *144* (4), 1556−1571.
(32) Zhou, H.; Li, Z.; Xu, S. M.; Lu, L.; Xu, M.; Ji, K.; Ge, R.; Yan, Y.; Ma, L.; Kong, X.; Zheng, L.; Duan, H. Selectively Upgrading Lignin Derivatives to Carboxylates through Electrochemical Oxidative C-(OH)-C Bond Cleavage by a Mn-Doped Cobalt Oxyhydroxide Catalyst. *Angew. Chem., Int. Ed.* **2021**, *60* (16), 8976−8982.
(33) Hu, Q.; Gao, K.; Wang, X.; Zheng, H.; Cao, J.; Mi, L.; Huo, Q.; Yang, H.; Liu, J.; He, C. Subnanometric Ru clusters with upshifted D band center improve performance for alkaline hydrogen evolution reaction. *Nat. Commun.* **2022**, *13* (1), 3958.
(34) Li, Z.; Li, X.; Zhou, H.; Xu, Y.; Xu, S. M.; Ren, Y.; Yan, Y.; Yang, J.; Ji, K.; Li, L.; Xu, M.; Shao, M.; Kong, X.; Sun, X.; Duan, H. Electrocatalytic synthesis of adipic acid coupled with H2 production enhanced by a ligand modification strategy. *Nat. Commun.* **2022**, *13* (1), 5009.
(35) Amouzegar, K.; Savadogo, O. Electrocatalytic hydrogenation of phenol on highly dispersed Pt electrodes. *Electrochim. Acta* **1994**, *39* (4), 557−559.
(36) Amouzegar, K.; Savadogo, O. Electrocatalytic hydrogenation of phenol on dispersed Pt: Effect of metal electrochemically active surface area and electrode material. *J. Appl. Electrochem.* **1997**, *27* (5), 539−542.
(37) Amouzegar, K.; Savadogo, O. Electrocatalytic hydrogenation of phenol on dispersed Pt: reaction mechanism and support effect. *Electrochim. Acta* **1998**, *43* (5), 503−508.
(38) Song, Y.; Gutiérrez, O. Y.; Herranz, J.; Lercher, J. A. Aqueous phase electrocatalysis and thermal catalysis for the hydrogenation of phenol at mild conditions. *Appl. Catal., B* **2016**, *182*, 236−246.
(39) Liu, W.; You, W.; Gong, Y.; Deng, Y. High-efficiency electrochemical hydrodeoxygenation of bio-phenols to hydrocarbon fuels by a superacid-noble metal particle dual-catalyst system. *Energy Environ. Sci.* **2020**, *13* (3), 917−927.
(40) Wijaya, Y. P.; Grossmann-Neuhaeusler, T.; Dhewangga Putra, R. D.; Smith, K. J.; Kim, C. S.; Gyenge, E. L. Electrocatalytic Hydrogenation of Guaiacol in Diverse Electrolytes Using a Stirred Slurry Reactor. *ChemSusChem* **2020**, *13* (3), 629−639.
(41) Wijaya, Y. P.; Smith, K. J.; Kim, C. S.; Gyenge, E. L. Synergistic effects between electrocatalyst and electrolyte in the electrocatalytic reduction of lignin model compounds in a stirred slurry reactor. *J. Appl. Electrochem.* **2021**, *51* (1), 51−63.
(42) Felicetti, T.; Cannalire, R.; Pietrella, D.; Latacz, G.; Lubelska, A.; Manfroni, G.; Barreca, M. L.; Massari, S.; Tabarrini, O.; Kieć-Kononowicz, K.; Schindler, B. D.; Kaatz, G. W.; Cecchetti, V.; Sabatini, S. 2-Phenylquinoline S. aureus NorA Efflux Pump Inhibitors: Evaluation of the Importance of Methoxy Group Introduction. *J. Med. Chem.* **2018**, *61* (17), 7827−7848.
(43) Peng, T.; Zhuang, T.; Yan, Y.; Qian, J.; Dick, G. R.; Behaghel de Bueren, J.; Hung, S.-F.; Zhang, Y.; Wang, Z.; Wicks, J.; Garcia de Arquer, F. P.; Abed, J.; Wang, N.; Sedighian Rasouli, A.; Lee, G.; Wang, M.; He, D.; Wang, Z.; Liang, Z.; Song, L.; Wang, X.; Chen, B.; Ozden, A.; Lum, Y.; Leow, W. R.; Luo, M.; Meira, D. M.; Ip, A. H.; Luterbacher, J. S.; Zhao, W.; Sargent, E. H. Ternary Alloys Enable Efficient Production of Methoxylated Chemicals via Selective Electrocatalytic Hydrogenation of Lignin Monomers. *J. Am. Chem. Soc.* **2021**, *143* (41), 17226−17235.
(44) Wang, M.; Peng, T.; Yang, C.; Liang, B.; Chen, H.; Kumar, M.; Zhang, Y.; Zhao, W. Electrocatalytic hydrogenation of lignin monomer to methoxy-cyclohexanes with high faradaic efficiency. *Green Chem.* **2022**, *24* (1), 142−146.
(45) Han, S.; Zhang, X.; Wang, R.; Wang, K.; Jiang, J.; Xu, J. Electrocatalytic conversion of G-type and S-type phenolic compounds from different tree species in a heteropolyacid fluidized system. *Chem. Eng. J.* **2023**, *452*, 139299.
(46) Chin, D. T.; Vilambi, N. R. K.; Cheng, C. Y. Oxidation of phenol to benzoquinone in a CSTER with modulated alternating voltage. *J. Appl. Electrochem.* **1989**, *19* (3), 459−461.
(47) Han, C.; Ye, Y.; Wang, G.; Hong, W.; Feng, C. Selective electro-oxidation of phenol to benzoquinone/hydroquinone on polyaniline enhances capacitance and cycling stability of polyaniline electrodes. *Chem. Eng. J.* **2018**, *347*, 648−659.
(48) Sprang, F.; Herszman, J. D.; Waldvogel, S. R. Electrochemical oxidation of phenols in flow: a versatile and scalable access to para-benzoquinones. *Green Chem.* **2022**, *24* (13), 5116−5124.
(49) Xu, W.; Sun, Y.; Li, N.; Liu, W.; Zhang, Z. C. Copper and Cobalt Co-catalyzed Selective Electrooxidation of Phenol to p-Benzoquinone Under Mild Conditions. *ChemElectroChem.* **2023**, *10* (18), No. e202300187.
(50) Xu, H.; Liu, X.; Zhao, Y.; Wu, C.; Chen, Y.; Gao, X.; Liu, Z. Reductive Cleavage of C—O Bond in Model Compounds of Lignin. *Chin. J. Chem.* **2017**, *35* (6), 938−942.
(51) Zhai, Q.; Han, S.; Wang, K.; Jiang, J.; Xu, J. Electrocatalytic cleavage of aryl ether C-O linkages in lignin model dimers. *Fuel Process. Technol.* **2022**, *235*, 107350.
(52) Garedew, M.; Young-Farhat, D.; Bhatia, S.; Hao, P.; Jackson, J. E.; Saffron, C. M. Electrocatalytic cleavage of lignin model dimers using ruthenium supported on activated carbon cloth. *Sustainable Energy & Fuels* **2020**, *4* (3), 1340−1350.
(53) Mahdavi, B.; Lafrance, A.; Martel, A.; Lessard, J.; MéNard, H.; Brossard, L. Electrocatalytic hydrogenolysis of lignin model dimers at Raney nickel electrodes. *J. Appl. Electrochem.* **1997**, *27* (5), 605−611.
(54) Song, Y.; Chia, S. H.; Sanyal, U.; Gutiérrez, O. Y.; Lercher, J. A. Integrated catalytic and electrocatalytic conversion of substituted phenols and diaryl ethers. *J. Catal.* **2016**, *344*, 263−272.
(55) Yang, C.; Magallanes, G.; Maldonado, S.; Stephenson, C. R. J. Electro-reductive Fragmentation of Oxidized Lignin Models. *J. Org. Chem.* **2021**, *86* (22), 15927−15934.
(56) Wang, R.; Kang, Y.; Wu, J.; Jiang, T.; Wang, Y.; Gu, L.; Li, Y.; Yang, X.; Liu, Z.; Gong, M. Electrifying Adipic Acid Production: Copper-Promoted Oxidation and C-C Cleavage of Cyclohexanol. *Angew. Chem., Int. Ed.* **2022**, *61* (50), No. e202214977.
(57) Huang, J.; Jian, Y.; Zhou, M.; Wu, H. Oxidative C-C bond cleavage of lignin via electrocatalysis. *Front. Chem.* **2022**, *10*, 1007707.
(58) Chen, J.; Yang, H.; Fu, H.; He, H.; Zeng, Q.; Li, X. Electrochemical oxidation mechanisms for selective products due to C-O and C-C cleavages of beta-O-4 linkages in lignin model compounds. *Phys. Chem. Chem. Phys.* **2020**, *22* (20), 11508−11518.
(59) Bender, M. T.; Warburton, R. E.; Hammes-Schiffer, S.; Choi, K.-S. Understanding Hydrogen Atom and Hydride Transfer Processes during Electrochemical Alcohol and Aldehyde Oxidation. *ACS Catal.* **2021**, *11* (24), 15110−15124.
(60) Bender, M. T.; Lam, Y. C.; Hammes-Schiffer, S.; Choi, K. S. Unraveling Two Pathways for Electrochemical Alcohol and Aldehyde Oxidation on NiOOH. *J. Am. Chem. Soc.* **2020**, *142* (51), 21538−21547.
(61) Bosque, I.; Magallanes, G.; Rigoulet, M.; Karkas, M. D.; Stephenson, C. R. J. Redox Catalysis Facilitates Lignin Depolymerization. *ACS Cent. Sci.* **2017**, *3* (6), 621−628.

https://doi.org/10.1021/prechem.4c00024
Precis. Chem. 2024, 2, 428−446

(62) Rafiee, M.; Alherech, M.; Karlen, S. D.; Stahl, S. S. Electrochemical Aminoxyl-Mediated Oxidation of Primary Alcohols in Lignin to Carboxylic Acids: Polymer Modification and Depolymerization. *J. Am. Chem. Soc.* **2019**, *141* (38), 15266−15276.
(63) Yan, K.; Zhang, Y.; Tu, M.; Sun, Y. Electrocatalytic Valorization of Organosolv Lignin Utilizing a Nickel-Based Electrocatalyst. *Energy Fuels* **2020**, *34* (10), 12703−12709.
(64) Ouyang, D.; Gao, D.; Qiang, Y.; Zhao, X. Highly-efficient conversion of lignin to electricity by nickel foam anode loaded with solid electrocatalysts. *Appl. Catal., B* **2023**, *328*, 122491.
(65) Badalyan, A.; Stahl, S. S. Cooperative electrocatalytic alcohol oxidation with electron-proton-transfer mediators. *Nature* **2016**, *535* (7612), 406−410.
(66) Monos, T. M.; Magallanes, G.; Sebren, L. J.; Stephenson, C. R. J. Visible light mediated reductions of ethers, amines and sulfides. *J. Photochem. Photobiol., A* **2016**, *328*, 240−248.
(67) Du, X.; Liu, W.; Zhang, Z.; Mulyadi, A.; Brittain, A.; Gong, J.; Deng, Y. Low-Energy Catalytic Electrolysis for Simultaneous Hydrogen Evolution and Lignin Depolymerization. *ChemSusChem* **2017**, *10* (5), 847−854.
(68) Wei, L.; Guo, S.; Yan, G.; Chen, C.; Jiang, X. Electrochemical pretreatment of heavy oil refinery wastewater using a three-dimensional electrode reactor. *Electrochim. Acta* **2010**, *55* (28), 8615−8620.
(69) Stiefel, S.; Lölsberg, J.; Kipshagen, L.; Möller-Gulland, R.; Wessling, M. Controlled depolymerization of lignin in an electrochemical membrane reactor. *Electrochem. commun.* **2015**, *61*, 49−52.
(70) Ma, L.; Zhou, H.; Kong, X.; Li, Z.; Duan, H. An Electrocatalytic Strategy for C-C Bond Cleavage in Lignin Model Compounds and Lignin under Ambient Conditions. *ACS Sustain. Chem. Eng.* **2021**, *9* (4), 1932−1940.
(71) Cai, P.; Fan, H.; Cao, S.; Qi, J.; Zhang, S.; Li, G. Electrochemical conversion of corn stover lignin to biomass-based chemicals between Cu/Ni-Mo-Co cathode and Pb/PbO2 anode in alkali solution. *Electrochim. Acta* **2018**, *264*, 128−139.
(72) Carmo, M.; Fritz, D. L.; Mergel, J.; Stolten, D. A comprehensive review on PEM water electrolysis. *Int. J. Hydrog. Energy* **2013**, *38* (12), 4901−4934.
(73) Wang, Y.-s.; Yang, F.; Liu, Z.-h.; Yuan, L.; Li, G. Electrocatalytic degradation of aspen lignin over Pb/PbO2 electrode in alkali solution. *Catal. Commun.* **2015**, *67*, 49−53.
(74) Lu, X.; Wang, J.; Peng, W.; Li, N.; Liang, L.; Cheng, Z.; Yan, B.; Yang, G.; Chen, G. Electrocatalytic hydrogenation of phenol by active sites on Pt-decorated shrimp shell biochar catalysts: Performance and internal mechanism. *Fuel* **2023**, *331*, 125845.
(75) Garedew, M.; Young-Farhat, D.; Jackson, J. E.; Saffron, C. M. Electrocatalytic Upgrading of Phenolic Compounds Observed after Lignin Pyrolysis. *ACS Sustain. Chem. Eng.* **2019**, *7* (9), 8375−8386.
(76) Gu, Z.; Zhang, Z.; Ni, N.; Hu, C.; Qu, J. Simultaneous Phenol Removal and Resource Recovery from Phenolic Wastewater by Electrocatalytic Hydrogenation. *Environ. Sci. Technol.* **2022**, *56* (7), 4356−4366.
(77) Zhou, Y.; Gao, Y.; Zhong, X.; Jiang, W.; Liang, Y.; Niu, P.; Li, M.; Zhuang, G.; Li, X.; Wang, J. Electrocatalytic Upgrading of Lignin-Derived Bio-Oil Based on Surface-Engineered PtNiB Nanostructure. *Adv. Funct. Mater.* **2019**, *29* (10), 1807651.
(78) Zhou, L.; Zhu, X.; Su, H.; Lin, H.; Lyu, Y.; Zhao, X.; Chen, C.; Zhang, N.; Xie, C.; Li, Y.; Lu, Y.; Zheng, J.; Johannessen, B.; Jiang, S. P.; Liu, Q.; Li, Y.; Zou, Y.; Wang, S. Identification of the hydrogen utilization pathway for the electrocatalytic hydrogenation of phenol. *Sci. China Chem.* **2021**, *64* (9), 1586−1595.
(79) Du, Y.; Chen, X.; Liang, C. Selective electrocatalytic hydrogenation of phenols over ternary Pt3RuSn alloy. *Mol. Catal.* **2023**, *535*, 112831.
(80) Cui, T.; Ma, L.; Wang, S.; Ye, C.; Liang, X.; Zhang, Z.; Meng, G.; Zheng, L.; Hu, H. S.; Zhang, J.; Duan, H.; Wang, D.; Li, Y. Atomically Dispersed Pt-N3C1 Sites Enabling Efficient and Selective Electrocatalytic C-C Bond Cleavage in Lignin Models under Ambient Conditions. *J. Am. Chem. Soc.* **2021**, *143* (25), 9429−9439.
(81) Ko, M.; Pham, L. T. M.; Sa, Y. J.; Woo, J.; Nguyen, T. V. T.; Kim, J. H.; Oh, D.; Sharma, P.; Ryu, J.; Shin, T. J.; Joo, S. H.; Kim, Y. H.; Jang, J.-W. Unassisted solar lignin valorisation using a compartmented photo-electro-biochemical cell. *Nat. Commun.* **2019**, *10* (1), 5123.

https://doi.org/10.1021/prechem.4c00024
Precis. Chem. 2024, 2, 428−446